Analysis of neuronal transcripts of PGC-1α transgenic mice

Julia Maria Döhla

Master's Thesis

Master's Degree Programme in Translational Medicine

Faculty of Medicine

University of Helsinki

2013

Faculty of Medicine	Master's Degree Programme in Translational Medicine	
Subject: Translational medicine	Master's thesis	
Author Julia Maria Döhla		
Title Analysis of neuronal transcripts of PGC-1α transgenic mice		
Supervisor Professor Dan Lindholm	Month and year April 2013	Number of pages 89
Supervisor's affiliation Department of Biochemistry and Developmental Biology, Institute of Biomedicine, University of Helsinki; Minerva Foundation Institute for Medical Research		

Abstract

Peroxisome proliferator activated receptor γ coactivator 1α (PGC-1α) is a transcriptional coactivator involved in mitochondrial biogenesis, oxidative stress response, and energy metabolism. PGC-1α is part of an energy sensing network that translates environmental influences into alterations in gene expression of mainly mitochondrial molecular pathways. A role in neuroprotection has been implicated for PGC-1α in the context of mitochondrial expression networks.

Our research group has previously established a transgenic mouse line with stable overexpression of PGC-1α in brain neurons. Transgenic overexpression of PGC-1α is associated with an enhanced functional state of mitochondrial energy production. In the context of neurodegenerative processes, brain neurons of PGC-1α transgenic mice are protected against oxidative stressors in the MPTP mouse model of Parkinson's Disease.

To further characterize the transcriptional activity of PGC-1α regulated gene networks in brains of transgenic mice, a quantitative real-time PCR based system was established. Gene expression was measured for a subset of genes found to be differentially regulated in a microarray based screening of RNA obtained from hippocampus and cortex of PGC-1α transgenic mice.

Increased PGC-1α gene expression was found in hippocampus and cortex of PGC-1α transgenic mice, and their translation into protein was confirmed immunohistochemically. Expression analysis revealed significant changes in mRNA levels of PGC-1α controlled molecular pathways involved in mitochondrial energy production and antioxidant responses. Furthermore, alterations in the expression of some non-mitochondrial genes with established links to neurodegeneration were observed. Furthermore, a change in $GABA_A$ receptor subunit expression was detected.

In accordance with previous studies on the PGC-1α transgenic mouse line, these findings suggest that differential gene expression associated with PGC-1α overexpression contributes to an enhanced functional state of neurons in hippocampus and cortex of PGC-1α transgenic mice.

Increased knowledge about the transcriptional modulation of neuronal genes regulated by PGC-1α can lead to better insights into mechanisms governing neurodegeneration and neuroprotective pathways. Pharmacological modulation of PGC-1α activity may be a feasible approach for neuroprotective treatments in neurodegenerative diseases, such as Parkinson's Disease.

Keywords
Mitochondria, molecular pathways, neurodegeneration, neuroprotection, Parkinson's Disease, PGC-1α, qPCR

Where deposited

Additional information

Table of Contents

Abbreviations

–	qPCR program run without extension time during the amplification step
+	qPCR program run with extension time during the amplification step
°C	degrees Celsius
Acetyl-CoA	Acetyl coenzyme A
Acly	Citrate lyase
ADP	Adenosine diphosphate
AMPK	AMP (adenosine monophosphate)-activated kinase
AS	antisense
Atg3	Autophagocytosis associated protein 3
ATP	Adenosine triphosphate
Atp5h	ATP synthase, H+ transporting, mitochondrial F0 complex, subunit d
cAMP	Cyclic adenosine monophosphate
cDNA	Complementary DNA
CoQ	Coenzyme Q
Cox5b	cytochrome c oxidase, subunit Vb
Cox7b	cytochrome c oxidase, subunit VIIb
COXIV	cytochrome c oxidase, subunit IV
Cp	quantification cycle
CREB	cAMP response element binding protein
Cx	cortex
CytC	cytochrome c
DA	dopaminergic
dH_2O	distilled water
DNA	deoxyribonucleic acid
dNTP	deoxynucleotide
E	Efficiency value
ERR α	Estrogen-related receptor
ETC	Electron transport chain
ETS	electron transport system
FADH	oxidized flavin adenine dinucleotide
$FADH_2$	reduced flavin adenine dinucleotide
GABA	γ–aminobutyric acid
$GABA_A$	γ–aminobutyric acid receptor A
Gabra2	$GABA_A$ receptor subunit α2
Gabrg2	$GABA_A$ receptor subunit γ2
GCN5	Lysine acetyltransferase 2A
GSH	reduced glutathione
Gsr	Glutathione reductase
GSSG	oxidized glutathione
Hc	Hippocampus
IHC	immunohistochemistry
IMM	inner mitochondrial membrane
mg	milligram
mM	millimolar
mm	millimeter
M-MLV	Modified murine leukemia virus
MnSOD	superoxide dismutase
MPP+	1-methyl-4-phenylpyridinium
MPTP	1-Methyl-4-phenyl-1,2,3,6-tetrahydropyridin
mRNA	messenger RNA
mTOR	Mammalian target of rapamycin
NAD^+	oxidized nicotinamide adenine dinucleotide

NADH	reduced nicotinamide adenine dinucleotide
Ndufa13	NADH dehydrogenase 1 alpha, subcomplex 13
Nedd8	Neural precursor cell expressed, developmentally down-regulated 8
NeuN	Rbfox3 RNA binding protein, fox-1 homolog (C. elegans) 3
NRF-1	Nuclear factor 1
NRF-2	Nuclear factor 2
PBS	phosphate buffered saline
PBS-T	phosphate buffered saline, supplemented with Triton-X
PCR	Polymerase chain reaction
PD	Parkinson's Disease
PGC-1α	Peroxisome proliferator activated receptor γ coactivator 1α
PKA	protein kinase A
PPARα	peroxisome proliferator activated receptor α
qPCR	quantitative real-time polymerase chain reaction
R	relative expression ratio
Rheb	Ras homolog enriched in brain
RNA	ribonucleic acid
ROS	Reactive oxygen species
rpm	revolutions per minute
RSV	resveratrol
S	sense
Sirt-1	Sirtuin 1 (silent mating type information regulation 2, homolog)
SNc	substantia nigra pars compacta
SOD2	superoxide dismutase 2
Stdev	standard deviation
tg	transgenic
Trx2	thioredoxin 2
TrxS-	oxidized thioredoxin
TrxSH	reduced thioredoxin
Uba3	ubiquitin-like modifier activating enzyme 3
UPS	ubiquitin-proteasome system
wt	wildtype
µg	microgram
µl	microliter
µm	micrometer

1. Review of the literature

1.1. Mitochondria

1.1.1. Mitochondrial energy metabolism

1.1.1.1. ATP production via cellular respiration

Mitochondria are cytosolic cell organelles harboring a number of the cell's most essential pathways for survival and energy metabolism. Mitochondria are critically involved in energy metabolism, being the site of adenosine triphosphate (ATP) production, and housing the pathways that regulate energy expenditure and storage on the level of the whole organism. *Reviewed in* (Duchen 2004, Nunnari, Suomalainen 2012)

One of the main functions of mitochondria is production of energy in form of ATP via oxidative phosphorylation in the electron transport chain (ETC) in a process known as cellular respiration. The ETC is a sequence of large enzyme complexes, whose subunits are encoded in a concerted way by the mitochondrial and nuclear genomes. As shown in figure 1, the enzymes are located within and spanning the mitochondrial inner membrane. *Reviewed in* (Duchen 2004, Nunnari, Suomalainen 2012, Abou-Sleiman, Muqit & Wood 2006, Schon, Przedborski 2011)

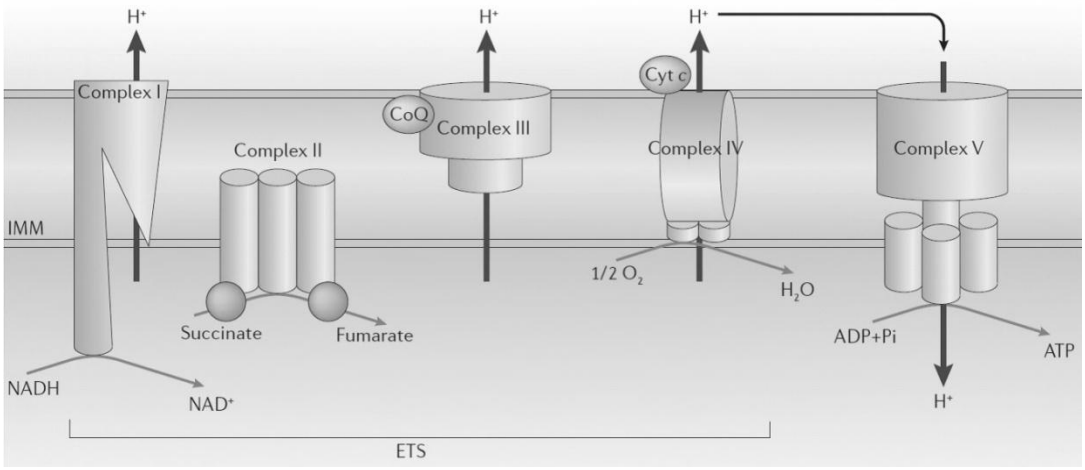

Figure 1 The mitochondrial electron transport chain. Shown here is the mitochondrial electron transport chain with electron transporting complexes I to IV and F_1F_O ATP synthase (complex V), the site of ATP production. Electrons are transported down the electron transport chain from complex I to IV, where they are transferred to oxygen to produce water. Redox reactions along complexes I to IV are building up a proton gradient that is used at complex V as driving force for phosphorylation of ATP. ETS: electron transport system, IMM: inner mitochondrial membrane, CoQ: coenzyme Q, Cyt C: cytochrome c. Reprinted by permission from Macmillan Publishers Ltd: Nature reviews. Neuroscience, (Abou-Sleiman, Muqit & Wood 2006)

The ETC function is based on the flow of electrons provided via metabolism of different nutrients. Breakdown of carbohydrates, proteins, and fatty acids results in production of acetyl coenzyme A (Acetyl-CoA), which enters the citric acid cycle. Via the citric acid cycle, metabolic pathways are integrated to yield the oxidized forms of the high energy compounds nicotinamide adenine dinucleotide (NADH) and flavin adenine dinucleotide ($FADH_2$). Both molecules act as electron carriers, and transfer electrons to ETC complexes I and II, respectively. Sequential transfer of energy in form of the received electrons along ETC complexes I to IV results in a series of redox reactions. At the end of a gradual oxidation of the ETC enzymes, electrons are transferred to molecular oxygen, resulting in reduction to water. With exception of complex II, the enzymes make use of the energetic flow to transfer protons across the inner membrane and into the inter-membrane space. Ultimately, the ETC enzymes' activity thereby generates a proton gradient across the mitochondrial inner membrane. (Duchen 2004)

This electrochemical gradient is utilized by complex V, the F_1F_o ATP synthase. The energy of a controlled backflow of electrons across the inner membrane allows complex V to generate ATP by phosphorylation of adenosine diphosphate (ADP). (Duchen 2004, Nunnari, Suomalainen 2012) ATP is redistributed throughout the cell to provide energy. (Schon, Przedborski 2011)

1.1.1.2. Regulation of mitochondrial energy metabolism

The activity of the ETC, reflecting the level of cellular respiration, is adapted to match the energetic needs of single cells as well as the whole organism. The ability of the mitochondrial respiratory chain to respond to alterations in the energy status, reflected by the ADP concentrations, and adapt the rate of ATP production to the energetic needs, is termed respiratory control. The regulatory mechanisms are coupled to the proton gradient across the mitochondrial inner membrane, and influenced by the availability of ADP, the energetic status and need for energy. *Reviewed in* (Duchen 2004, Nunnari, Suomalainen 2012)

1.1.2. Oxidant production and antioxidant system

During cellular respiration, reactive oxygen species (ROS) are generated as a by-product of electron transport chain activity. Leakage of unpaired electrons occurs during oxidative phosphorylation, mainly at complexes I and III. As a consequence of reactions between free electrons and oxygen, superoxide ions are generated. These are highly reactive oxidants, and can, in turn, be converted to other radical species and promote further formation of oxidants. (Nunnari, Suomalainen 2012, Kowaltowski et al. 2009, Turrens 2003)

Oxidants react with and thereby damage intracellular macromolecules, such as membrane lipids or DNA (deoxyribonucleic acid). Defects due to oxidative reactions can severely impair mitochondrial function and disturb the intracellular homeostasis. (Duchen 2004, Balaban, Nemoto & Finkel 2005, St-Pierre et al. 2006)

Mitochondria are the main producers of ROS, as well as the main targets of oxidative damage. Pronounced and sustained increases in respiratory activity can therefore entail a disturbance of the oxidant status, due to increased production of ROS.

In a physiological and functional state, mitochondria possess a well-developed system that allows them to scavenge most of the ROS before they can cause damage. An elaborate system of antioxidant defense mechanisms intrinsic to mitochondria scavenges the reactive molecules generated during cellular respiration (figure 2 shows a summary of the antioxidant systems immediately scavenging ROS). Among these defense systems, the most prominent are glutathione, superoxide dismutases, thioredoxin, and catalase. Acting on different stages of oxidant production allows these systems to maintain a low level of oxidants. (Duchen 2004, Kowaltowski et al. 2009, Turrens 2003, Lin, Beal 2006)

Glutathione, for example, serves to scavenge reactive oxidant species by reducing them to a more stable state, thereby preventing them from reacting with and damaging other intracellular molecules. This process leads to oxidation of glutathione and formation of glutathione disulfide. The functionality of the glutathione antioxidant system is regenerated by the enzyme glutathione reductase that maintains the pool of glutathione in a steady-state. (Nicholls 2002)

In addition, mitochondrial uncoupling proteins can partly dissipate the proton gradient, allowing protons to cross the membrane independently of ATP production. By reducing the electrochemical gradient, uncouplers decrease the production of ROS via the respiratory chain complexes. (Duchen 2004, Andrews, Diano & Horvath 2005)

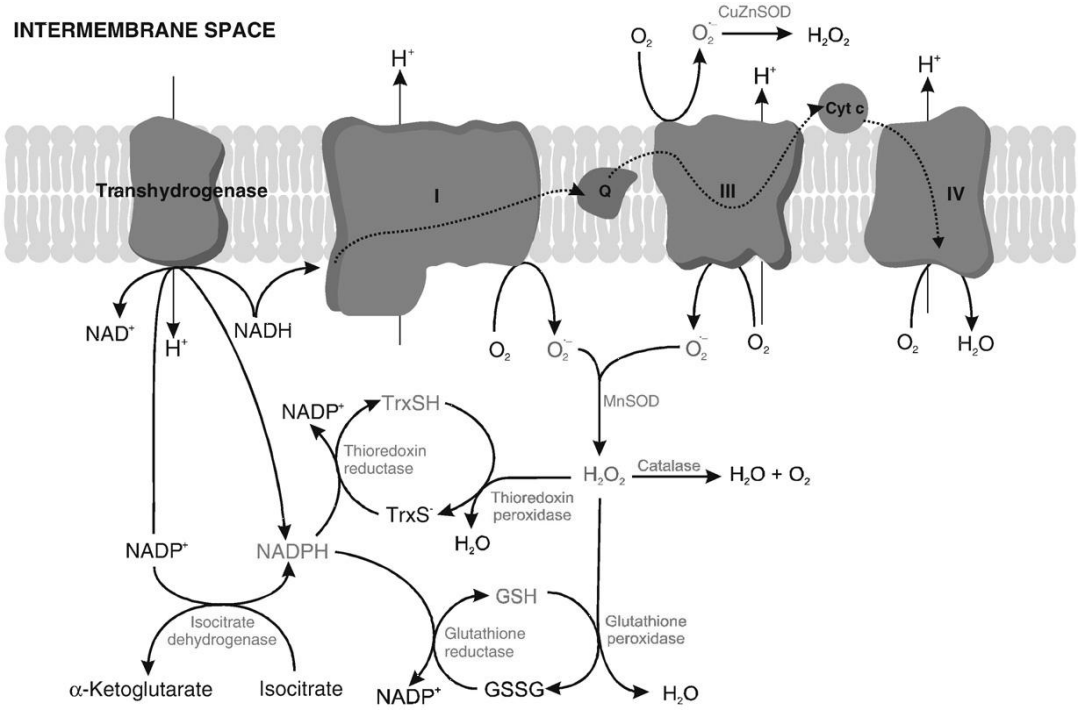

Figure 2 Mitochondrial oxidant production, antioxidant systems and ROS scavenging. Complexes I and III are the main sites of reactive oxygen species (ROS) production. Shown here are the main steps in ROS scavenging in immediate proximity to the electron transport chain. ROS are dismutated by MnSOD superoxide dismutase. The main immediate ROS scavengers are catalase, and the peroxidases thioredoxin peroxidase and glutathione peroxidase. Antioxidants thioredoxin and glutathione are oxidized to buffer ROS, and reductases (thioredoxin reductase, glutathione reductase) maintain the functionality of antioxidants. GSH: reduced glutathione, GSSG: oxidized glutathione, MnSOD: superoxide dismutase, TrxSH: reduced thioredoxin, TrxS-: oxidized thioredoxin. Reprinted by permission from Macmillan Publishers Ltd: Free radical biology & medicine., (Kowaltowski et al. 2009)

1.2. Role of mitochondria in neurodegenerative diseases, as exemplified by Parkinson's Disease

1.2.1. Parkinson's Disease

1.2.1.1. Clinical features of Parkinson's disease

Parkinson's disease (PD) is a neurodegenerative disorder predominantly affecting dopminergic neurons of the nigrostriatal pathway. This midbrain pathway connects the striatum to substantia nigra pars compacta (SNc) and is important for the

initiation of voluntary movements. Degeneration of the nigrostriatal pathway results in a decreased dopaminergic input to the striatum, complicating movement coordination.

Due to the importance of this pathway's functionality in movement initiation, movements of PD patients typically appear slow and rigid. Further clinical symptoms of PD are resting tremor, postural instability, and bradykinesia. Common non-motor symptoms are autonomic and cognitive dysfunction. More rarely, patients also develop psychological symptoms, such as depression and dementia. *Reviewed in* (Jankovic 2008, Poewe 2008, Schapira et al. 2009, Dexter, Jenner 2013)

Preclinical symptoms with an onset earlier during disease progression are rather unspecific and therefore often remain unrecognized or undiagnosed for a long time. In most cases, the clinical symptoms only become overt when up to 60% of dopaminergic (DA) neurons of the nigrostriatal pathway have already been lost. At this time point, neurodegenerative processes have been progressing for years or even decades. (Dauer, Przedborski 2003, Schapira 2009)

This delay in diagnosis hampers effective treatment, since neurons, once lost, cannot be replaced or regenerated with the currently used treatments. Dopamine-replacement therapies, such as levodopa-administration, are to date the gold standard of PD medication. However, they can alleviate the symptoms only for a limited time frame, without being able to actually protect the remaining neuronal population from degeneration or restore neuronal capacity that has already been lost. With these merely symptomatic treatments, it is at present impossible to restore functionality of the nigrostriatal system. To date, there is no curative treatment for PD neurodegeneration. (Dexter, Jenner 2013) In order to improve the outcome, it would be crucial to start treatments already early in disease progression. The second challenge is the development of neuroprotective drugs – this approach then could slow or possibly even halt the demise of neurons. (Schapira 2009)

1.2.1.2. Molecular pathogenesis of Parkinson's Disease

In PD pathogenesis, DA neurons of the nigrostriatal pathway undergo cell death in a dying back process: degeneration of neuron terminals in the striatum is followed by demise of cell bodies located in SNc. (Dauer, Przedborski 2003)

There is no single cause for this degenerative process and its specificity for the nigrostriatal pathway. Rather, a cascade of events under mutual influence affects the functionality of this neuronal population. (Jenner, Olanow 2006) To date, it is not known which of the events involved in neuronal death is to be considered the initial trigger for degeneration, if this first step towards disease progression exists at all. Rather, findings have been pointing towards a more integrative explanation. (Jenner, Olanow 2006)

There are a number of specific defects that have been associated with Parkinsonism:

Mutations in a number of genes have been identified in association with familial cases of PD, such as α-synuclein or parkin. The disruption of cellular functions caused by those mutations is causative for Parkinsonism. (Thomas, Beal 2007, Thomas, Beal 2011)

Moreover, several neurotoxins have been reported to cause Parkinsonism in a clinical context, and are also used to model Parkinsonism in animal models. (Betarbet et al. 2000, Przedborski et al. 2004) Interestingly, most of the gene mutations and neurotoxic assaults target processes involved in mitochondrial function.

Apart from these specific assaults, age is the most influential contributor to PD risk. The reasons for this are still not fully understood, but numerous factors also known to be contributing to the physiological aging process are involved in neurodegeneration in general and neuronal demise in PD, in particular. (Beal 2005) Strikingly, most of the pathways considered contributors to neurodegenerative processes are linked to mitochondria.

It has been proposed that decreasing mitochondrial functionality is one of the most important key factors promoting disease risk. (Lin, Beal 2006) Mitochondrial metabolism, oxidative state and biogenesis are emerging as pivotal influences on neuronal functionality. In case of a deregulation of the tightly maintained homeostasis, these processes can turn into triggers for neuronal dysfunction and severely disturb mitochondrial and neuronal functionality. Impaired functionality, in turn, contributes to further accumulation of cellular damage, and neurons enter a cycle of progressive damage. Ultimately, this interferes with the cells' ability to maintain a functional state, and leads to neuronal death. (Dauer, Przedborski 2003)

The cause of degeneration of DA neurons in the nigrostriatal pathway is thought to be impaired functionality of a number of interconnected and tightly linked processes and, most importantly, the mutual influences among these processes. The dysregulations and nonfunctional state of these pathways seem to be cause and consequence at the same time – disturbances in either of the pathways is reinforced by previous disruptions of the functional state. These disturbances, in turn, further propel the derangement of cellular homeostasis. Regardless of what the initial pathogenic event has been, over the course of disease development, neurons are trapped in a spiral of increasing and self-promoting disruption of homeostasis and damage. (Jenner, Olanow 2006, Thomas, Beal 2007)

Among the most prominent contributors to cell death in PD are mitochondrial dysfunctions. However, a number of processes not linked to mitochondria are involved in pathogenesis as well. (Jenner, Olanow 2006, Thomas, Beal 2007, Jenner 2003) In the following sections, I am going to review the main mitochondrial and non-mitochondrial factors that together unsettle the functional state of neurons.

1.2.2. Mitochondria in neurodegenerative pathogenesis

1.2.2.1. Importance of mitochondria in neurons

With their functions in energy metabolism, antioxidant systems and regulation of cell death, mitochondria are crucial for all cells. Some characteristics of neurons, however, make them even more dependent on mitochondrial processes.

First of all, the high energy demands and metabolic activity typical for neurons have to be met constantly. In addition, most of the ATP consumed by neurons is generated through oxidative metabolism, using glucose. For these reasons, neurons are critically dependent on mitochondrial ETC activity and energy production. This energetic profile and high respiratory activity entails the production of large quantities of ROS via the ETC. As a consequence, the mitochondrial antioxidant system has to be maintained in a highly functional state to ensure constantly low ROS levels. (Nicholls et al. 2007)

In addition, neuronal signaling processes depend on the maintenance of tightly regulated balances in ion concentrations, such as calcium, involved in synaptic signal transmission and regulated by mitochondrial buffering. These processes are

particularly important and have to be kept at a tightly regulated balance in neurons. (Nicholls et al. 2007, Murphy, Fiskum & Beal 1999, Arduino et al. 2010)

1.2.2.2. Mitochondrial processes in neurodegenerative pathogenesis

For the reasons reviewed above, neurons are more vulnerable towards disturbances in the balance regulating mitochondrial functions and cellular homeostasis.

In case of pronounced increases in production of ROS during cellular respiration, the mitochondrial antioxidative defense mechanisms are overwhelmed and oxidants accumulate. This state is known as oxidative stress, and characterized by the presence of higher than normal amounts of ROS. The surplus of oxidants in the cell, in turn, causes further oxidative reactions harming macromolecules. Cells enter a cycle of ever increasing damage, while the ability to scavenge oxidants is progressively being impaired. At long last, this processes amounts to a dysfunctional state of mitochondrial energy production. (Murphy, Fiskum & Beal 1999)

Under conditions of bioenergetic failure, oxidative stress impairs mitochondrial processes involved in energy metabolism, and in particular, the respiratory chain. The functionality and efficiency of ATP production via the electron transport chain is impaired, predominantly due to oxidative damage to complex I. This complex is among the main sites of electron leakage, and, especially in an impaired functional state, propels the production of ROS. (Betarbet et al. 2000) As a consequence, the electrochemical gradient maintained by means of managing proton concentrations on either side of the mitochondrial inner membrane cannot be kept at a stable level. The membrane tends to depolarize and the proton gradient partially dissipates. This causes a drop in the driving force for ATP production, and the energy metabolism via oxidative phosphorylation cannot be maintained on a level sufficient to meet the needs of the cell and organism. Bioenergetic failure links energy metabolism and oxidative stress. Together, these impairments lead to a state of mitochondrial dysfunction. Ultimately, this entails severe disturbances within the cellular functionality, leading to cell death. (Schon, Przedborski 2011, Beal 2003, Schulz et al. 2000)

Furthermore, cellular pathways involved in the regulation of recycling of dysfunctional cell components, cell death and survival are affected during disease

progression. (Abou-Sleiman, Muqit & Wood 2006) Autophagy, the process of lysosomal degradation of organelles, has been implicated in neurodegeneration. Nonfunctional cell organelles are taken up into autophagosomes. Subsequently, autophagosomes fuse with lysosomes, where organelles are degraded or partially recycled. Autophagy is regulated via protein modifications, and influenced by a number of signaling pathways also involved in regulation of cellular survival, for example in mammalian target of rapamycin (mTOR) signaling. (Kim, Rodriguez-Enriquez & Lemasters 2007, Lee, Giordano & Zhang 2012)

In addition, glutamate mediated excitotoxicity contributes to the demise of neurons in PD. Excitotoxicity is defined as a pronounced overstimulation of neurons via glutamate-signaling. Excessive calcium-influx entails disturbances in several cellular processes and damage to macromolecules. Eventually, these disturbances trigger apoptotic cell death. (Jenner, Olanow 2006, Blandini 2010)

Disturbances of homeostasis in several cellular processes render neurons more vulnerable to excitotoxic assaults. Under oxidative stress conditions, neurons are more likely to undergo calcium overload. The balance of intracellular calcium levels becomes more fragile, and in case of even mild glutamatergic overstimulation, the depolarization balance can easily be tilted towards initiation of excitotoxic cell death. This process is linked to mitochondria, which have an important role in maintaining the calcium homeostasis. (Duchen 2004, Blandini 2010, Atlante et al. 2001, Beal 1998, Meredith et al. 2008, Meredith et al. 2009, Surmeier et al. 2011)

Under conditions of increased oxidative stress, the ubiquitin-proteasome system (UPS), which controls the degradation of misfolded and nonfunctional proteins, is overloaded by the large amount of damaged molecules. In a healthy state, the UPS serves to identify and scavenge misfolded or otherwise nonfunctional proteins. If refolding into the appropriate conformation by chaperones does not succeed, damages proteins are degraded via the proteasome. A histological hallmark of PD is the presence of Lewy bodies, inclusions of α-synuclein in the cytoplasm of affected neurons. Again, it is not known whether these inclusions contribute to neurodegeneration or serve as a storage compartment for misfolded proteins. (Thomas, Beal 2011, Moore et al. 2005, Schapira 2008)

An additional process triggered by increased oxidative conditions is inflammation. During late stages of disease progression, inflammation further increases the oxidative stress in the remaining neurons' environment. (Surmeier et al. 2011, Schapira 2008, Cohen, Farooqui & Kesler 1997, Cohen 2000, Cowell, Blake & Russell 2007, Tritos et al. 2003)

DA neurons are thought to be affected by the initial increase in oxidative stress levels more than other cells, among other reasons due to excessive oxidant production as a byproduct of dopamine metabolism. (Lotharius, Brundin 2002) After onset of neuronal demise, remaining functional DA neurons compensate with increased dopamine production in order to maintain the functional state of the nigrostriatal system. Increased dopamine turnover via monoamine oxidase, in turn, entails even further increase in oxidant production. (Zigmond, Hastings & Perez 2002, Brotchie, Fitzer-Attas 2009, Spina, Cohen 1989)

Taken together, oxidative stress and mitochondrial dysfunction are emerging as important contributors to degeneration of neurons in PD. All of the pathways reviewed above are linked and contribute to PD pathogenesis in a concerted way. (Jenner 2003, Murphy, Fiskum & Beal 1999, Cohen 2000, Jenner 2004)

Ultimately, the interactions and mutual influences of the factors reviewed above may determine the way in which the tightly regulated homeostasis among numerous pathways is disturbed and gradually unsettle the physiological state of neurons. (Jenner, Olanow 2006) This again may be decisive for the vulnerability of particular cell populations, and, together with their biochemical and metabolic properties, target as well as restrict the demise of cells in PD to the particular population of DA neurons of the nigrostriatal pathway. (Cohen, Farooqui & Kesler 1997, Cohen 2000, Cohen, Kesler 1999a, Cohen, Kesler 1999b)

Together with the unique signaling properties of the nigrostriatal system, the interplay of disturbances in mitochondrial pathways affecting metabolism, oxidant production and scavenging may be one of the crucial factors conferring specificity to the neurodegenerative assaults. Initial disturbances may tip the well-balanced system of interlaced processes and pathways, causing an ever increasing and self-enhancing amount of oxidative stress and neuronal demise. The current view on pathogenesis assumes a number of events under mutual influence that lead to neuronal

degeneration in a concerted way. Rather than being caused by a single pathogenic event, neuronal degeneration results from a "circle" of events that all seem to be cause and consequence of neuronal demise at the same time – this underlines the complexity of pathogenic processes and shows how the neuronal physiology is profoundly disturbed. (Jenner, Olanow 2006, Jenner 2003, Surmeier et al. 2011, Lotharius, Brundin 2002)

At the intersection of the processes reviewed above, the transcriptional coactivator PGC-1α is emerging as the pivotal point controlling and integrating mitochondrial biogenesis and metabolism with the energetic and oxidative state of the cell. (Zheng et al. 2010)

1.3. Peroxisome proliferator activated receptor γ coactivator 1α (PGC-1α)

1.3.1. PGC-1α as a master regulator of mitochondrial pathways

Peroxisome proliferator activated receptor γ coactivator 1α (PGC-1α) is a transcriptional coactivator, and a master regulator of mitochondrial biogenesis, oxidative stress response, and, with its role in regulating respiration, of energy metabolism and homeostasis. (Kelly, Scarpulla 2004, Puigserver et al. 1998) reviewed in (Puigserver, Spiegelman 2003)

PGC-1α is a member of the PGC-1 coactivator family comprising some of the main regulators of adaptive responses to metabolic cues and environmental influences. The PGC-1 coactivators, and in particular PGC-1α, are in the center of a regulatory network of mainly mitochondrial metabolic adaptations to changes of energetic homeostasis. (Scarpulla 2011)

PGC-1α has been identified in the context of its role in adaptive thermogenesis in brown adipose tissue. (Puigserver et al. 1998) Subsequently, numerous additional processes have been found to be under the control of PGC-1α. Among these are metabolic responses to fasting, regulation of cellular respiration, glucose metabolism and energy homeostasis, regulation of mitochondrial generation of oxidants and antioxidant response, and mitochondrial biogenesis and turnover. PGC-1α has been studied extensively in brown adipose tissue, liver, skeletal muscle, heart, and brain. (St-Pierre et al. 2006, Tritos et al. 2003, Clark, Simon 2009, Esterbauer et al. 1999, Lin, Handschin & Spiegelman 2005, St-Pierre et al. 2003, Tsunemi, La Spada 2012)

All these tissues are highly dependent on oxidative metabolism and a closely regulated maintenance of energy supply. (Lin, Handschin & Spiegelman 2005)

The variety of cellular processes that are regulated by or in some manner influenced via PGC-1α and downstream effectors points out the importance of this regulatory circuit and is as perplexing as the number of environmental cues that either have a direct impact on PGC-1α activity or indirectly trigger PGC-1α mediated responses. This points out the integrative function PGC-1α has within a nutrient sensing network maintaining energetic and oxidative balance, and coordinating the regulation of metabolic adaptation. (Lin, Handschin & Spiegelman 2005)

PGC-1α is, first of all, expressed in a tissue specific manner. (Puigserver et al. 1998, Esterbauer et al. 1999) Furthermore, expression is regulated in response to environmental influences that restrict the availability of nutrients. As a consequence, intracellular cyclic adenosine monophosphate (cAMP) levels increase, and the transcription factor cAMP response element binding protein (CREB) is activated by protein kinase A (PKA). Together with other transcription factors, CREB induces expression of PGC-1α. (Lin, Handschin & Spiegelman 2005)

PGC-1α is also directly activated in response to environmental stimuli and energetic alterations via posttranscriptional modifications. (Arduino et al. 2010, Scarpulla 2011, Fernandez-Marcos, Auwerx 2011, Jeninga, Schoonjans & Auwerx 2010) Within this regulation network, the deacetlyase sirtuin (silent mating type information regulation 2 homolog) 1 (Sirt-1) functions as an immediate activator of PGC-1α activity. (Canto, Auwerx 2009) Sirt-1 belongs to a family of deacetlyases whose activity is dependent on intracellular NAD+ levels as well as NAD+/NADH and AMP/ATP ratios, reflecting the nutrient state of a cell. (Imai et al. 2000) Energy deprivation increases Sirt-1 activity via a number of integrative signaling pathways. Sirt-1 decreases the acetylation levels of PGC-1α, which leads to an immediate activation of PGC-1α. PGC-1α is inactivated by acetylation via lysine acetyltransferase 2A (GCN5) under conditions of increased nutrient availability. (Nunnari, Suomalainen 2012, Fernandez-Marcos, Auwerx 2011, Jeninga, Schoonjans & Auwerx 2010) The regulatory network of PGC-1α activity in response to nutrient status is summarized in figure 3.

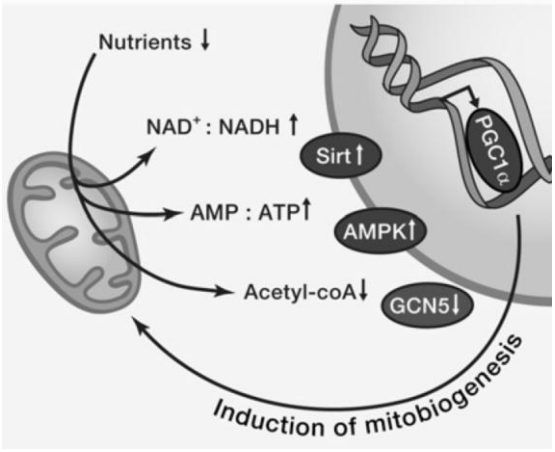

Figure 3 PGC-1α in the center of a mitochondrial nutrient sensing network. PGC-1α expression and activity are regulated via a network of mitochondrial sensors in dependence of the energetic status if the cell. Upon nutrient depletion, NAD+/NADH and AMP/ATP ratios rise, whereas acetyl-CoA concentrations decrease. This activates Sirt-1 and AMP (adenosine monophosphate)-activated kinase (AMPK), which leads to enhanced expression and activation of PGC-1α. Deactivation of PGC-1α is mediated by lysine acetyltransferase 2A (GCN5) under conditions of high nutrient availability. NAD+/NADH: nicotinamide adenine dinucleotide, oxidized and reduced form, AMP: adenosine monophosphate, ATP: adenosine triphosphate. Reprinted by permission from Macmillan Publishers Ltd: Cell, (Nunnari, Suomalainen 2012)

Apart from expression regulation, the specificity of PGC-1α targeting certain genes is partly conferred by interaction with transcription factors and their tissue specific expression patterns. As a coactivator of transcription, PGC-1α regulates and coordinates gene expression networks by interacting with a number of transcription factors, such as nuclear factors NRF-1 and NRF-2, and estrogen-related receptor ERR α. (Puigserver et al. 1998, Clark, Simon 2009, Wu et al. 1999, Mootha et al. 2004, Scarpulla 2006)

These transcription factors target a number of nuclear encoded mitochondrial genes: among the main expression networks under PGC-1α control are mitochondrial respiratory chain complexes and other enzymes involved in cellular respiration. (Lin, Handschin & Spiegelman 2005, Rohas et al. 2007)

On a broader level, gene expression networks encoding for proteins promoting mitochondrial biogenesis depend on PGC-1α. Taken together, PGC-1α activation and increased expression of downstream networks results in an increased mitochondrial number per cell, as well as enhanced functional capacity of mitochondria. (Wareski et al. 2009)

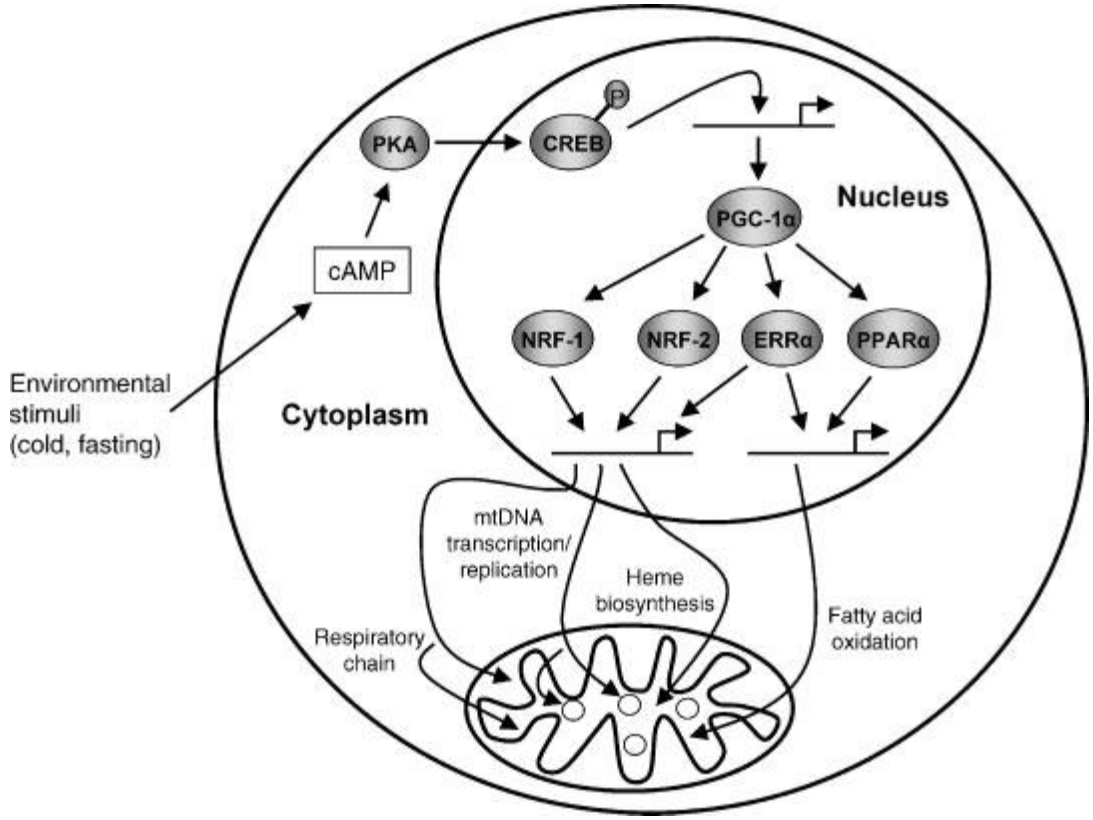

Figure 4 PGC-1α in the center of regulatory networks translating environmental influences to transcriptional responses. PGC-1α expression is induced in response to environmental stimuli influencing energetic status, transduced by changes in cyclic AMP (cAMP) levels via protein kinase A (PKA) and the transcription factor CREB (cAMP response element-binding protein). PGC-1α in turn acts as coactivator of a number of transcription factors to enhance mitochondrial biogenesis and pathways involved in energy metabolism. NRF-1: nuclear factor 1, NRF-2: nuclear factor 2, ERRα: estrogen-related receptor, PPARα: peroxisome proliferator-activated receptor α. Reprinted by permission from Macmillan Publishers Ltd: Journal of Cellular Biochemistry, (Scarpulla 2006)

Due to the higher mitochondrial respiration rate upon PGC-1α activation, the amounts of ROS generated as byproducts of oxidative phosphorylation also rise. Potentially harmful consequences of enhanced metabolic activity are as well counteracted via PGC-1α. In parallel with enhancing energy metabolism, PGC-1α stimulates the expression of mitochondrial antioxidants. This leads to a boost in the functional state of the oxidant scavenging system and retains the homeostasis. (St-Pierre et al. 2006) This mechanism of immediate maintenance of low intracellular oxidant levels is essential for oxidative species management. PGC-1α regulated networks allow for increasing metabolic activity without consequential damage due to higher reactive oxygen levels. (St-Pierre et al. 2006, Zheng et al. 2010, Clark, Simon 2009, Lin, Handschin & Spiegelman 2005, St-Pierre et al. 2003, Kukidome et al. 2006, Valle et al. 2005)

1.3.2. PGC-1α in neuronal function

While initially studied in brown adipose tissue, skeletal and heart muscle, and liver, the functional impact of PGC-1α on brain neurons has recently been coming into focus. All of the tissues critically dependent on PGC-1α functions are highly oxidative. In line with this, PGC-1α is an essential regulator of energy and oxidative stress homeostasis in neurons. (Wareski et al. 2009) PGC-1α expression is being increased in response to oxidative stress challenges and mediates the antioxidant system maintaining neuronal homeostasis. In contrast, cells lacking functional PGC-1α are neither able to adequately react to oxidative stress nor to regulate energy homeostasis. (St-Pierre et al. 2006, Zheng et al. 2010, Lin et al. 2004)

A number of studies have proven the essential function of PGC-1α in mitochondrial biogenesis and regulation, maintaining energy homeostasis and matching ATP production to the cellular need while also maintaining a low level of oxidative stressors in an integrative signaling network. PGC-1α has repeatedly been linked to neuroprotection and neurodegeneration. (St-Pierre et al. 2006, Zheng et al. 2010, Kelly, Scarpulla 2004, Puigserver, Spiegelman 2003, Lin et al. 2004, Scarpulla 2002, Mudo et al. 2012, Leone et al. 2005)

In the following sections, I am going to review evidence for an essential function of PGC-1α in neurons, particularly with focus on the role of PGC-1α in neurodegenerative diseases and PD.

1.3.3. PGC-1α in neuroprotection and neurodegeneration

1.3.3.1. Clinical implications for a role of PGC-1α in Parkinson's Disease

Alterations in the expression of PGC-1α have been implicated as one of the underlying factors for neurodegenerative processes, and, in particular, PD pathogenesis. In a large meta-analysis of independent microarray based gene expression studies, Zheng and colleagues identified gene sets associated with PD. (Zheng et al, 2010)

As a basis, Zheng and coworkers used gene expression studies on autopsy samples, including results based on analysis of different brain areas as well as selective studies of DA neurons. A number of gene set showing differential expression

patterns in PD patients with clinical as well as subclinical disease status as compared to healthy controls were identified. Underexpression of gene sets encoding biological functions was considered an indication for the respective pathways being affected during PD pathogenesis. Among the underexpressed gene sets, Zheng et al report a high prevalence of gene expression networks controlled by PGC-1α. Among the genes identified to be associated with PD, a substantial fraction was being contributed by molecular pathways involved in mitochondrial metabolism. Gene sets comprising the entire set of nuclear encoded electron transport chain subunits were found to be underexpressed in samples of subclinical as well as clinically prevalent PD. This holds true for DA neurons as well as non-nigral neurons. Other deregulated pathways that were identified by this study include several mitochondrial pathways involved in different stages of energy metabolism (predominantly glucose utilization based), and mitochondrial biogenesis and protein handling.

A striking common feature of these pathways underexpressed in PD patients is their responsiveness to PGC-1α regulation. PGC-1α controlled networks were found to be defective and underexpressed in both substantia nigra as well as non-nigral tissues. The initial screening results were identified for these gene sets using quantitative real-time polymerase chain reaction (qPCR), and differential expression at low levels was detected association with in subclinical as well as clinical PD.

Zheng and coworkers show that dysregulations in the gene expression levels of PGC-1α regulated networks, particularly those involved in mitochondrial energy metabolism and biogenesis, are strongly associated with PD and may be crucially contributing to disease development. (Zheng et al. 2010)

Taking into consideration that PGC-1α is known to have a positive impact on the functional state of mitochondria, and to regulate energy homeostasis and metabolism in neurons, these clinical findings strongly suggest a crucial role of PGC-1α in neuroprotection against degenerative processes. (Wareski et al. 2009)

1.3.3.2. Studies in model systems: Loss of PGC-1α

Neuroprotective features of PGC-1α mediated gene expression networks have been studied in different model systems *in vitro* and *in vivo*. Studies of the effects of depletion of functional PGC-1α in cell culture as well as in mouse models have

helped identify downstream gene expression networks under the regulation of PGC-1α. (St-Pierre et al. 2006, Wu et al. 1999, Rohas et al. 2007, Valle et al. 2005)

Two independent reports characterizing stable PGC-1α null mouse lines have provided further evidence for the importance of PGC-1α in maintaining energetic and oxidative state homeostasis in brain neurons. Furthermore, these studies provide further evidence for dysregulations of PGC-1α mediated gene expression networks in neurodegenertion. (St-Pierre et al. 2006, Lin et al. 2004, Leone et al. 2005)

Both of the PGC-1α depleted mouse models are based on whole body knockout of functional PGC-1α, resulting in a complete depletion of PGC-1α mRNA (messenger RNA, ribonucleic acid) and protein levels. PGC-1α knockout mice are viable, but suffer from abnormalities linked to disturbances in energy metabolism. Transgenic (tg) mice are unable to adapt their body temperature upon cold exposure, confirming the crucial involvement of PGC-1α in adaptive thermogenesis. (St-Pierre et al. 2006, Lin et al. 2004, Leone et al. 2005)

Furthermore, mitochondrial oxidative phosphorylation is less efficient in liver and skeletal muscle of PGC-1α null mice. This suggests essential functions of PGC-1α and downstream metabolic networks in mitochondrial metabolism. (Leone et al. 2005)

Both PGC-1α null mouse lines showed structural abnormalities in the central nervous system. More specifically, lesions in several brain regions, including hippocampus (Hc) and cortex (Cx) were reported by both groups. St-Pierre et al also report lesions resembling neurodegenerative lesions in the striatum of tg mice. Additional neurodegenerative lesions were found in different brain areas. (St-Pierre et al. 2006, Lin et al. 2004, Leone et al. 2005) These findings are due to neuronal disruption of PGC-1α signaling, as proven by similar findings in mice with neuron-specific knockout of PGC-1α, which develop comparable patterns of neurodegenerative lesions. (Ma et al. 2010)

PGC-1α null mice exhibit pronounced changes in movement behavior, presumably due to disruption by the above described brain lesions. Signaling pathways are known to be disrupted in some of the brain regions affected in PGC-1α null mice also in human neurodegenerative diseases, predominantly in PD. This leads to the hypothesis that PGC-1α obtains an essential function in neuroprotection and

disruption of PGC-1α mediated signaling pathways is a crucial feature of neurodegeneration. (St-Pierre et al. 2006, Lin et al. 2004, Leone et al. 2005)

Further characterization of the neurodegenerative lesions and consequences for functional state and health of PGC-1α null mice central nervous system was performed with the 1-Methyl-4-phenyl-1,2,3,6-tetrahydropyridin (MPTP) mouse model of PD. (St-Pierre et al. 2006) MPTP is a precursor form of the neurotoxin 1-methyl-4-phenylpyridinium (MPP+). MPTP is metabolized to its active form in glial cells and partly in neurons, and MPP+ is selectively taken up by the dopamine transporter into DA neurons, where it inhibits complex I of the mitochondrial respiratory chain. This causes an increase in the amount of ROS that is produced during the cellular respiration. (Przedborski et al. 2004)

MPTP is widely used as a model for neurodegenerative processes similar to those seen in PD. *Reviewed in* (Winklhofer, Haass 2010) In wildtype (wt) as well as PGC-1α null mice, MPTP causes a reduction in the number of DA neurons in parallel with an increase in oxidative stress levels. MPTP induced neurodegeneration is associated with increased levels of oxidative damage, predominantly in substantia nigra. PGC-1α knockout mice show more pronounced loss of TH-positive DA neurons in the substantia nigra than controls. (St-Pierre et al. 2006)

Excitotoxicity in the context of PGC-1α depletion has also studied in PGC-1α null mice. Kainic acid is used as a model for oxidative stress via excitotoxic mechanisms, and known to confer excitotoxic damage to hippocampal neurons via an increase of oxidative stress. The increased vulnerability of brain neurons lacking PGC-1α also holds true under excitotoxic conditions: PGC-1α null mice are more susceptible towards excitotoxic stress than wt controls. (Wang et al. 2005)

The higher vulnerability of PGC-1α depleted neurons towards excitotoxic and oxidative stress assaults shows an essential role of PGC-1α in neuroprotection against similar processes. Further characterization of neurons under PGC-1α depletion using gene expression analysis revealed underexpression of genes linked to mitochondrial oxidative phosphorylation. In line with this, skeletal muscle cells of PGC-1α null mice show reduced expression levels of a number of genes involved in mitochondrial electron transport chain, ATP production and energy metabolism. In

addition, expression of mitochondrial antioxidants was shown to be decreased in the brains of PGC-1α null mice. (St-Pierre et al. 2006)

1.3.3.2. Studies in model systems: Gain of PGC-1α

The fact that loss of PGC-1α is clinically correlated with neurodegeneration as well as the findings provided by studies in PGC-1α null mice point towards a strong role of PGC-1α in neuroprotection. In order to study the effects of increased PGC-1α levels in neurons, my colleagues have established a mouse line with stable overexpression of PGC-1α in brain neurons (Mudo et al. 2012).

The PGC-1α tg mouse line expresses flag-tagged exogenous PGC-1α under the control of the neuron-specific Thy1.2 promoter. This renders the expression of exogenous PGC-1α specific to brain neurons. The Thy1.2 promoter is activated after birth, and remains driving expression of PGC-1α from then on. (Vidal et al. 1990, Caroni 1997) Expression of exogenous PGC-1α results in increased protein levels in different brain areas of the tg mice, as reported for substantia nigra, pars compacta (SNc) and striatum. (Mudo et al. 2012)

In order to study possible neuroprotective properties conferred by PGC-1α overexpression, tg mice were treated with the neurotoxin MPTP. As reviewed in chapter 1.3.3.2., MPTP causes oxidative stress in DA neurons by means of inhibition of complex I of the mitochondrial respiratory chain. This allows studying disturbances in cellular physiology similar to those in neurons under neurodegenerative assaults in PD.

Unlike wt control mice, where MPTP causes a pronounced decrease in the number of TH positive DA neurons in the substantia nigra, PGC-1α tg mice are almost completely resistant towards this oxidative stressor. Upon MPTP treatment, the number of viable TH-positive DA neurons does not undergo significant changes in PGC-1α tg mice, and equally, the overall number of neurons remains stable upon MPTP treatment. In addition, the functional state of the nigrostriatal system was found to be enhanced in PGC-1α tg mice, measured as improved dopamine metabolism.

This shows that PGC-1α overexpression renders DA neurons of the nigrostriatal system less susceptible towards oxidative assaults. Together with the findings of an

increased vulnerability of PGC-1α null mice towards MPTP mediated neurodegeneration, the strong neuroprotective function of PGC-1α overexpression indicates an essential role of endogenous PGC-1α expression and signaling in neuroprotection.

In order to study the mechanisms underlying the neuroprotection mediated by PGC-1α, gene expression in brains of PGC-1α tg mice was assessed. The mitochondrial antioxidants superoxide dismutase 2 (SOD2) and thioredoxin 2 (Trx2) are present at higher levels in the SNc of tg mice. This enhanced expression is accompanied by a rise in mRNA for SOD2.

Furthermore, the respiratory control ratio was found to be enhanced in mitochondria purified from whole brain extracts of PGC-1α tg mice, as compared to wt controls, showing an improved capacity for ATP production and mitochondrial energy metabolism in neurons of PGC-1α tg mice. In line with this, expression levels of mRNA encoding the subunit IV of mitochondrial eletron transport chain complex IV were found to be increased in substantia nigra of tg mice. This change in transcriptional activity was also reflected by increased protein levels.

These results show that PGC-1α overexpression causes functional alterations in the expression of mitochondrial genes involved in energy metabolism and oxidative stress scavenging pathways. These changes lead to an enhanced response to oxidative stress, which may increase the capability of DA neurons to scavenge oxidative assaults and thereby contribute to enhancing cell viability under oxidative conditions. PGC-1α overexpression enhances the functional state of mitochondrial energy production and improves the neurons' ability to maintain energy homeostasis.

Taken together, the findings reported by Mudò et al strongly suggest a role of PGC-1α in contributing to the control of oxidative stress response and a neuroprotective role of PGC-1α against processes as observed in PD. (Mudo et al. 2012)

1. 4. GABAergic signaling and implications of PGC-1α

γ-aminobutyric acid (GABA) is one of the main inhibitory neurotransmitters in the brain, with most of the fast synaptic inhibitory signaling being mediated by $GABA_A$ receptors. $GABA_A$ receptors are ionotropic receptor channels with selectivity for

anions. In brain neurons, GABA-mediated opening mostly allows an influx of chloride, which stabilizes the membrane potential close to the resting potential. This decreases the probability of depolarization, and has a physiological role predominantly in inhibitory postsynaptic signaling.

$GABA_A$ receptors are pentameric receptors composed of different combinations of α, β, and γ subunits. Subunit composition varies depending on the function and location of the receptors and influences the functional properties of the receptors.

$GABA_A$ receptors mediate mainly synaptic, phasic and fast inhibition. In addition, however, they also contribute to extrasynaptic, tonic inhibitory signaling. The location and functionality of a receptor is determined by its subunit composition and depends on neuronal activity. (Hines et al. 2012, Holopainen, Lauren 2003, Purves 2012)

Alterations in $GABA_A$ receptor subunit composition have been reported in context of neuronal demise, and GABAergic signaling has been associated with protective properties against excitotoxicity. Particularly, enhanced GABA mediated inhibition can protect neurons from excitotoxic cell death, as studied after stroke. (Hines et al. 2012)

Localization of PGC-1α to GABAergic neurons and regulatory networks have been studied in rat brains. During development of the rat brain, most GABAergic neurons were found to express PGC-1α. Equally, in mature rat brains, PGC-1α was found to be strongly expressed in hippocampal and cortical GABAergic neurons. (Cowell, Blake & Russell 2007)

Functional properties of inhibitory interneurons in hippocampus, cortex, and striatum of PGC-1α depleted mice undergo changes, due to alterations in expression patterns of proteins involved in calcium-signaling. It is thought that these changes have an impact on GABA release and may impair inhibitory signaling properties. It has been suggested that PGC-1α depletion is associated with interneuron pathology in neurodegeneration. (Lucas et al. 2010)

Furthermore, studies in PGC-1α knockout mice suggest that PGC-1α expression in GABAergic neurons has an essential function role in neuronal protection from excitotoxicity, possibly due to maintenance of energetic homeostasis and neuroprotection via antioxidants. (Cowell, Blake & Russell 2007, Lucas et al. 2010)

1.5. Quantitative real-time PCR

Quantitative real-time PCR (qPCR) is based on the exponential amplification of a DNA template during PCR reaction. By thermal cycling, DNA template conformation is repeatedly altered from single- to double stranded, and, during amplification reactions characterized by ideal temperature conditions for firstly, primer annealing to a target sequence within the DNA template and, secondly, amplification of this sequence by a heat-stable DNA polymerase. The newly synthesized double stranded products are separated by a steep increase in temperature and can subsequently serve as templates during the next amplification cycle. In order to render the amount of double stranded PCR product measurable, a fluorescent dye, in this Master's thesis study SYBR Green, is added to the initial reaction. SYBR Green intercalates unspecifically in double stranded DNA. Binding to DNA causes SYBR Green to undergo a conformational change, which in turn leads to a pronounced increase in fluorescence emission. In consequence, fluorescence levels directly reflect the amount of double stranded DNA. *Reviewed in* (VanGuilder, Vrana & Freeman 2008)

In a qPCR setup, this principle is utilized by measuring the fluorescence intensity repeatedly throughout the reaction and thereby monitoring the amplification of template. Amplification specificity for a targeted gene is conferred by specific primers. During the amplification reaction, the amount of PCR-product increases exponentially, with (under ideal conditions) a doubling of reaction product during each cycle. By following the fluorescence increase during the PCR reaction, the quantification cycle (Cp) value can be determined. The Cp value is defined as the number of amplification cycles that is needed until the fluorescence intensity crosses a preset threshold value and is clearly discernible from background fluorescence. (Schmittgen, Livak 2008) It thus is indirectly correlated with the initial template copy number in the starting reaction, as it reflects the presence of a sufficient copy number of product for fluorescence to cross the threshold. The number of amplification cycles required until the Cp value is reached allows conclusions about the initial amount of a template (determined by the primer sequence specificity) in the starting reaction. Comparing Cp values for the same template for reactions containing complementary DNA (cDNA) of different samples allows for calculating the relative amounts of template present in the initial reactions. This approach is

widely used to measure relative gene expression levels of target genes. A well-established method, used in this Master's Thesis study, is the ΔΔCp method for relative quantification. (Schmittgen, Livak 2008, Pfaffl 2001, Livak, Schmittgen 2001)

This method is based on reverse transcription of mRNA to cDNA, with the mRNA directly reflecting the transcriptional activity upon target genes. During reverse transcription, the relative abundances of transcripts for individual genes are maintained. The cDNA population that is used as input for qPCR therefore reflects the mRNA population and expression levels. *Reviewed in* (Dorak 2006)

Figure 5 shows a representative amplification course for qPCR reactions. In the example, the expression level of a target gene is to be compared between tg and control samples. Amplification of the target gene specific transcript yields Cp values for both samples. To render the obtained Cp values comparable, expression is, in a first step, normalized to one or several reference genes. These are genes known to be expressed at stable levels among varying conditions and not being influenced by changes in the expression of other genes. Commonly, gene expression levels of genes of interest are given as a relative value in dependence on the expression of reference genes. (Pfaffl 2001, Dorak 2006)

In a qPCR setup, amplification reactions for the reference genes are performed in parallel to the reactions for the target genes. Cp values of reference genes in tg and control sample are subtracted from the corresponding Cp values for the target genes. This normalization yields the ΔCp value for both the tg and the control sample (compare figure 5). ΔCp, or the expression differences between target and reference gene, is a relative value for the level of gene expression of the target gene, as compared to the stable expression level of a reference gene. (Pfaffl 2001, Dorak 2006)

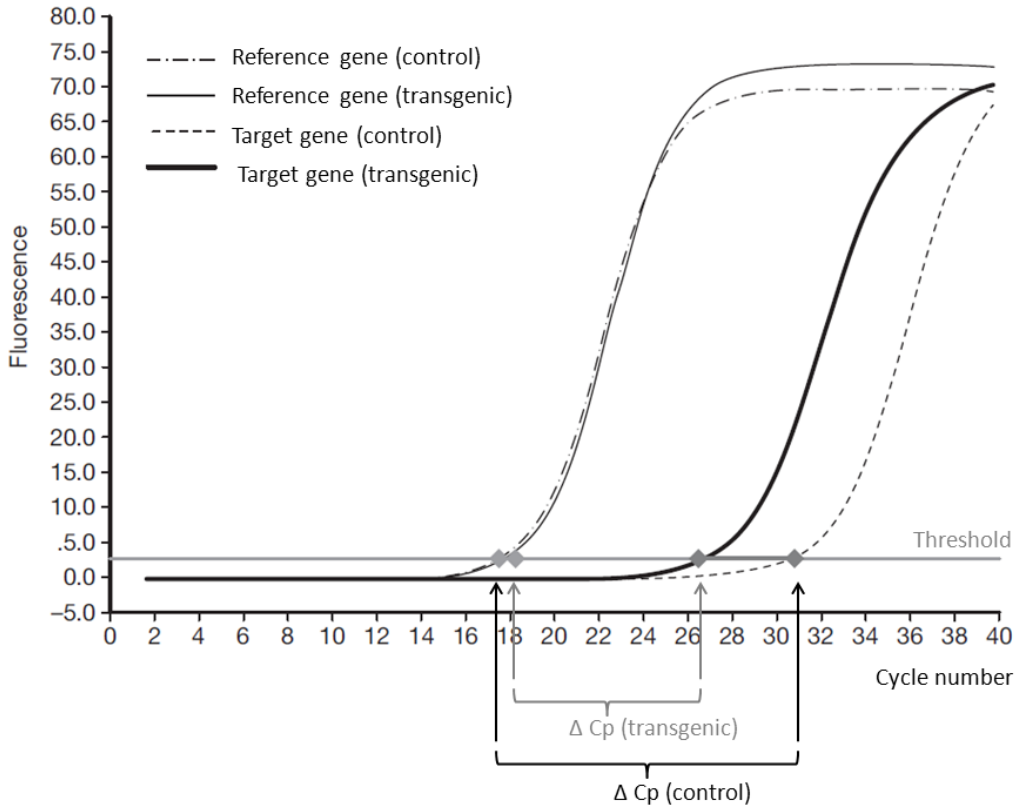

Figure 5 **Principle of relative gene expression measurement with the ΔΔCp method for relative quantificatio**n. Adapted from (Dorak 2006)

The difference between the ΔCp values for transgenic and control samples reflects the difference in expression levels between the samples. Under ideal reaction conditions, the relative expression ratio (R) is given as follows (Livak, Schmittgen 2001):

$$R = 2^{-[\Delta Cp_{transgenic} - \Delta Cp_{control}]} = 2^{-\Delta\Delta Cp}$$

In order to ensure reliability, the calculation is adapted to take into account differences between the reaction efficiencies for different genes. Calculation of relative gene expression of a target gene in the transgenic sample, normalized to the expression of a reference gene, is then summarized in the following formula, *adapted from* (Dorak 2006):

$$Relative\ gene\ expression = \frac{(E_{target})^{\Delta Cp_{target}}}{(E_{reference})^{\Delta Cp_{reference}}}$$

$$\Delta Cp = Cp\ (control) - Cp(transgenic)$$

E describes the efficiency value (calculation of efficiencies is described in chapter 4.1.2.), which is a measure for the dynamic development of the amplification reaction. Under optimal reaction conditions, the efficiency of a qPCR reaction equals 2.0, which corresponds to a perfect doubling of input DNA template during each amplification cycle. (Pfaffl 2001, Dorak 2006)

2. Aims of the study

This Master's Thesis study is based on the transgenic mouse line established by Mudò et al. (Mudo et al. 2012) Aims of this study were to further characterize the transgenic mouse line in order to identify functional alterations and gene expression networks associated with overexpression of PGC-1α.

Previously, a microarray based screening was performed, and revealed differential gene expression in hippocampus and cortex of PGC-1α transgenic mice. From the differentially regulated genes, a subset of genes was chosen for further study. These included genes encoding mitochondrial proteins known to be part of metabolic and regulatory pathways with established links to PD pathogenesis.

For this, I established a qPCR based system for reassessment of differential gene expression in wildtype and PGC-1α transgenic mouse brains. Immunohistochemistry supplemented the analysis with expression studies at the protein level.

3. Materials and methods

3.1. Workflow of the analysis

Transgenic mice of the PGC-1α overexpressing strain created and described by Mudò et al were in the focus of this Master's Thesis study. C57BL/6J mice (The Jackson Laboratory, Bar Harbor, ME, USA) were chosen as wt controls in accordance with the genetic background of the tg mice. (Mudo et al. 2012)

Mice of the tg strain express flag-tagged PGC-1α under the control of the neuron-specific Thy1.2 promoter. (Vidal et al. 1990, Caroni 1997) Tg mice were genotyped at an age of approximately three weeks.

For analysis of the gene expression levels, eight week old male mice were sacrificed and tissues (Hc and Cx) were excised. RNA extraction was performed with the RNeasy Lipid Tissue Mini Kit (QIAGEN, Hilden, Germany). This method is based on a phenol chloroform extraction followed by column based purification of RNA. After quantification of the yield and quality control, RNA was used for cDNA synthesis using SuperScript VILO cDNA Synthesis Kit (Invitrogen, Carlsbad, CA, USA).

cDNA was used for quantitative real time PCR on a Roche LightCycler 480 II (Roche Diagnostics, Basel, Switzerland) with the SybrGreen method of quantification. qPCR was performed to study the expression levels of 14 genes of interest, chosen based on the results of a microarray (GeneChip Mouse Exon ST Array, Affymetrix, Santa Clara, CA, USA), performed earlier in our research group.

3.2. Genotyping

Tg mice were genotyped for expression of exogenous PGC-1α at an age of three weeks using ear tissue samples. For tissue lysis, samples were incubated at 96ºC in 75µl of buffer containing 25mM NaOH and 0.2mM EDTA for 45 minutes (min) and briefly cooled on ice. The reaction was stopped by adding 75µl of a 40mM Tris-solution (pH 8).

Genotyping was performed with a PCR assay targeting the exogenous PGC-1α gene. Per single reaction, 5µl of DNA-extract was added to a Master Mix consisting of 5µl F-518 5x Phusion HF Reaction Buffer (Thermo Scientific, Waltham, MA, USA),

0.5µl dNTP mix (10mM, Thermo Scientific, Waltham, MA, USA), 1µl each sense (S) and antisense (AS) primer (20µM), 0.2µl F-530S Phusion DNA Polymerase 2U/µl (Thermo Scientific, Waltham, MA, USA) and 12.3µl dH_2O (distilled H_2O, BPC grade, Sigma Aldrich, Saint Louis, MO, USA) to a final volume of 25µl.

PCR for expression of exogenous PGC-1α was performed using the following primer sequences:

S 5'-CACTTCCTTGGCTTTCTCT-3', AS 5'-GTATCCAAGTCATTCACAT-3' (Thermo Scientific, Waltham, MA, USA).

The PCR reactions were incubated in Low Tube Strip Individual PCR Tubes (BioRad, Hercules, CA, USA) in a BioRad C1000 Thermal Cycler (BioRad, Hercules, CA, USA) under the following conditions:

		Temperature (ºC)	Time	
Denaturation		94	5min	
Amplification	Denaturation	94	60s	36 cycles
	Annealing	55	60s	
	Extension	72	60s	
		72	10min	

Table 1 PCR reaction conditions for genotyping.

PCR products were mixed with 6x DNA loading dye (Thermo Scientific, Waltham, MA, USA) and run on a 1% agarose gel (SeaKem LE agarose, Lonza, Basel, Switzerland) in 0.5x TBE buffer (44.5mM Tris, 44.5mM boric acid, 1.0mM EDTA, pH 8.0) containing SYBR Safe DNA gel stain (Invitrogen, Carlsbad, CA, USA) in a 1:10,000 dilution for visualization of DNA under UV light. 10µl DNA size standard (Quick-Load 100bp DNA Ladder or Quick-Load 100bp plus DNA Ladder, New England Biolabs, Ipswich, MA, USA) were loaded. Gels were run in 0.5x TBE buffer at 100V for 40-45 min on a PowerPac basic (BioRad, Hercules, CA, USA. PCR products resulted in bands of a lengths of 420bp, which were visualized under

UV light in an AlphaImager gel documentation system using AlphaImager Mini software (Protein Simple, Santa Clara, CA, USA).

3.3. RNA extraction

PGC-1α tg mice and wt controls were sacrificed at an age of eight weeks. Hippocampi and a tissue sample of the cortex were excised, taken up in ice cold RNAlater RNA Stabilization Reagent (QIAGEN AB, Hilden, Germany) and kept on ice to prevent degradation until RNA extraction was performed. The weight of the excised tissues ranged from 10 to 30mg.

RNA extraction was performed with the QIAGEN RNeasy Lipid Tissue Mini Kit (QIAGEN AB, Hilden, Germany) according to manufacturer's instructions. The workflow is based on a phenol-chloroform extraction of total RNA followed by silica-membrane based purification.

After transfer to reaction tubes containing ceramic beads (Precellys 24 Lysing Kit soft tissue homogenizing CK14, 1.4mm ceramic zirconium oxide beads in 0,5mL or 2mL standard tubes, Bertin Technologies, Aix-en-Provence, France), tissue samples were homogenized in 500µl or 1000µl QIAzol Lysis Reagent (QIAGEN AB, Hilden, Germany). Tissues were homogenized by operating the samples at 6,500rpm for 45s twice with 15s intermediate break in a Precellys 24 tissue homogenizer (Bertin Technologies, Aix-en-Provence, France).

The homogenization step disrupts cellular membranes, promoting release of contents of the cytosol and cellular organelles into solution, and causes shearing of large molecules. QIAzol Lysis Reagent consists of phenol and guanidine thiocyanate. Guanidine thiocyanate is a chaotropic agent denaturating macromolecules. In addition, RNAses are inactivated. This contributes to protection of RNA from degradation. This lysis reagent is particularly suitable for extraction of nucleic acids from tissues with high fat contents, such as brain.

Homogenates were transferred to microreaction tubes and incubated at room temperature for 5min to facilitate access to nucleic acids by allowing dissociation of nucleoprotein complexes.

After formation of an emulsion with chloroform (Sigma-Aldrich, Saint Louis, MO, USA), samples were separated into three phases by a prolonged centrifugation step. During this process, RNA partitions to the upper, aqueous phase, which then was separated and used for further purification steps. In addition, the sample contains an intermediate phase in which DNA is concentrated, and an organic phase containing proteins and lipids.

The aqueous phase containing RNA was extracted and mixed with an equal amount (600µl, typically) of 70% ethanol in order to provide appropriate binding conditions for the following column purification steps. Spin columns provided with the kit contain a silica membrane to which all RNA molecules with a length of more than 200 bases are adsorbed. This enriches the sample for mRNA, since shorter RNAs are removed during purification. RNA remains attached during the subsequent washing steps using buffers provided with the kit, whereas purification reagents and contaminants are removed. RNA was eluted in 50µl RNAse-free water and stored at -70°C for further use.

RNA yield after purification was quantified photospectrometrically using a NanoVue plus spectrophotometer (GE Healthcare, Chalfont St Giles, Switzerland). Purity of RNA was assessed in dependence of the A260/A280 ratio, which allows ruling out protein contaminations in the sample.

3.4. cDNA synthesis

First-strand DNA for qPCR reactions was synthesized from the extracted RNA using the SuperScript VILO cDNA Synthesis Kit (Invitrogen, Carlsbad, CA, USA).

In a reverse transcription reaction, the RNA population was converted to cDNA subsequently serving as a starting template for qPCR reactions.

The SuperScript VILO cDNA Synthesis Kit contains a modified murine leukemia virus (M-MLV) reverse transcriptase. The reverse transcription reaction is dependent on binding of random primers to the purified RNA. Thereby, RNA obtained from the samples is transcribed to cDNA without affecting the ratios of RNAs in the sample. The cDNA used as input for qPCR thus reliably reflects the mRNA population as an average of the transcriptional activity in the sample cells.

As input for a 20µl reaction, 2.5µg RNA was used. For negative controls, RNA input was replaced with dH_2O (H_2O, BPC grade, Sigma Aldrich, Saint Louis, MO, USA). cDNA synthesis reactions were incubated in a BioRad C1000 Thermal Cycler (BioRad, Hercules, CA, USA) according to instructions provided with the kit, as summarized in the following table:

	Temperature (ºC)	Time (min)
Pre-incubation	25	10
cDNA synthesis	42	60
Termination of reaction	85	5

Table 2 Reaction conditions for cDNA synthesis.

cDNA was stored at -20°C until further use. Effective cDNA synthesis was assessed by performing PCR for actin β. cDNA diluted 1:10 in dH_2O (H_2O, BPC grade, Sigma Aldrich, Saint Louis, MO, USA) was used as input for the PCR reaction. Per single reaction, 2.5µl of diluted cDNA were added to 22.5µl Master Mix containing 5µl F-518 5x Phusion HF Reaction Buffer (Thermo Scientific, Waltham, MA, USA), 0.5µl deoxynucleotide (dNTP) mix (10mM each, Thermo Scientific, Waltham, MA, USA), 1µl each S and AS primer (20µM), 0.2µl F-530S Phusion DNA Polymerase 2U/µl (Thermo Scientific, Waltham, MA, USA) and 14.8µl dH_2O (H_2O, BPC grade, Sigma Aldrich, Saint Louis, MO, USA) to a final volume of 25µl. Negative controls containing undiluted cDNA negative control reactions instead of cDNA were run for every assay.

Primer sequences were: S 5' – CAC ACT GTG CCC ATC TAT GA – 3', AS 5' – CCA TCT CTT GCT CGA AGT CT – 3' (Sigma-Aldrich, Saint Louis, MO, USA).

PCR reactions were incubated in Thermo Scientific ABgene 0.5mL PCR Tubes (Thermo Scientific, Waltham, MA, USA) under the following conditions in a BioRad C1000 Thermal Cycler (BioRad, Hercules, CA, USA):

		Temperature (ºC)	Time	
Denaturation		95	10min	
Amplification	Denaturation	95	30s	31 cycles
	Annealing	60	30s	
	Extension	72	30s	
Reaction termination		72	10min	

Table 3 PCR reaction conditions for detection of actin β.

Under addition of 6x DNA loading dye (Thermo Scientific, Waltham, MA, USA), PCR products were loaded on a 1% agarose gel (SeaKem LE agarose, Lonza, Basel, Switzerland, in 0.5x TBE buffer) containing SYBR Safe DNA gel stain (Invitrogen, Carlsbad, CA, USA) and gels were run in 0.5x TBE buffer at 100V for 40-45 min on a PowerPac Basic (BioRad, Hercules, CA, USA). Size standards were Quick-Load 100bp DNA Ladder or Quick-Load 100bp plus DNA Ladder (New England Biolabs, Ipswich, MA, USA), of which 10µl were loaded. PCR products were visualized under UV light in an AlphaImager gel documentation system using AlphaImager Mini software (Protein Simple, Santa Clara, CA, USA) as bands of approximately 200bp.

3.5. Quantitative real-time PCR

SYBR Green I-based quantitative real-time PCR (qPCR) was performed on a Light Cycler 480 II Real-Time PCR System (Roche Diagnostics, Basel, Switzerland). Reactions were run in 96 well plate format (LightCycler 480 Multiwell Plate 96, white; 5x10 plates with sealing foils, Roche, Basel, Switzerland) with a final volume of 10µl per reaction.

All primers were obtained from Sigma-Aldrich (Saint Louis, MO, USA).

Actin β and GAPDH were used as reference genes. Primer sequences were: Actin β, S 5'-CCTTCTTGGGTATGGAATC-3', AS 5'- TGTTGGCATAGAGGTCTT-3', and GAPDH S 5'-CGACTTCAACAGCAACTC-3', AS 5'-TATTCATTGTCATACCAGGAA-3'.

Genes of interest were targeted using the following primer sequences:

Gene			Primer sequence (5'- 3')
Citrate lyase	Acly	S	TGAATACCGAGGACATTA
		AS	ATTGAATAGACCAGAGATG
Autophagocytosis associated protein 3	Atg3	S	AGATGGAGTATTCGGATGA
		AS	CCTGTAATACCTGTGTTGT
ATP synthase, H+ transporting, mitochondrial F0 complex, subunit d	Atp5h	S	AGAAGGAGGATGTGAAGA
		AS	TCAAGTCATCAATGGTCAT
Cytochrome c oxidase, subunit Vb	Cox5b	S	AAGGGACTGGACCCATAC
		AS	CACTATTCTCTTGTTGCTGATG
Cytochrome c oxidase, subunit VIIb	Cox7b	S	CGTGGTTATATTTGGAAT
		AS	GATTAAGGATTATGCTGAA
GABA receptor subunit α2	Gabra2	S	AACTAGACTTGGTTACTTT
		AS	TCTACTGTAAGCTCTACC
GABA receptor subunit γ2	Gabrg2	S	AATCCGTGGTTATTGTAA
		AS	GTATCTTGCTCAGTGTAA
Glutathione reductase	Gsr	S	GCATGATAAGGTACTGAG
		AS	TACTTCCTTAACCTGTGT
NADH dehydrogenase 1α, subcomplex 13	Ndufa13	S	CATGTGCCCACTCCCAAG
		AS	AGTCACTTCACAAGGCAGAAA
Neural precursor cell expressed, developmentally down-regulated 8	Nedd8	S	AGTGAAGAAACTTGGTTC
		AS	AGTAGACACACAAGATTG
Peroxisome proliferator-activated receptor gamma, coactivator 1α	PGC-1α	S	CAAACCAACAACTTTATC
		AS	TAGTCTTGTTCTCAAATG
Ras homolog enriched in brain	Rheb	S	GTTCCCTGGTTCTATTAAC
		AS	AACACGGAAGATAGAGAC
Sirtuin 1 (silent mating type information regulation 2, homolog)	Sirt-1	S	ATTGAAGATGCTGTGAAGTTAC TG
		AS	GGAGACAGAAACCCCAGC
Ubiquitin-like modifier activating enzyme 3	Uba3	S	TCACTCCAGTTCTTGTTAG
		AS	AACCAGATAATGCCAGATT

Table 4 Primer sequences for gene expression measurement using qPCR. S: sense primer, AS: antisense primer

Reaction conditions were optimized for each target gene to ensure most suitable reaction conditions and accuracy of quantification. As a first step, reaction conditions and primer concentrations were modified, if necessary, to obtain maximum specificity and sensitivity for individual primer pairs. This was followed by assessment of the reaction efficiencies for each gene. For the subsequent calculation of gene expression levels, amplification efficiencies were used as a parameter for the reaction rate of the PCR reaction. For a more detailed description of the optimization process, see chapter 4.1.

Measurements of gene expression levels were performed in reactions with a final volume of 10µl containing 5µl LightCycler 480 SYBR Green I Master (Roche, Basel, Switzerland), 2µl LightCycler 480 SYBR Green Master H_2O (Roche, Basel, Switzerland), 1µl primer mix, and 2µl cDNA, diluted 1:100 in dH_2O (H_2O, BPC grade, Sigma Aldrich, Saint Louis, MO, USA). Final cDNA dilution therefore was 1:500. Reactions were run in triplets, and no template controls (NTC), in which cDNA was replaced by LightCycler 480 SYBR Green Master H_2O (Roche, Basel, Switzerland), were included for each gene.

Expression levels in Hc and Cx of PGC-1α tg mice were determined in unpaired measurements in comparison to three wt controls for each of the genes of interest. All samples per target gene were measured within the same run to ensure comparable conditions for measurement. For each of the tg mice, measurements were repeated three to six times per tissue and gene of interest. In-run quality control was based on deviations of Cp values and analysis of melting temperature and dissociation curves. Biological replicates were measured within one run. Influence of sample position on the plate was assessed and position effects were excluded to ensure comparability between different runs.

Expression level calculations were performed based on the ΔΔCp method (as reviewed in chapter 1.5.). Gene expression values were normalized against the average of reference genes actin β and GAPDH. LightCycler analysis software (Roche Diagnostics, Basel, Switzerland) was used for calculations. For statistical analysis of significance levels, Student's T-test for paired measurements was performed. Significance levels for expression changes were assessed with one- and two-tailed T-test. P-values for directional changes in expression are given as calculated by one-tailed T-test.

Reaction conditions have been chosen based on prior optimization steps to ensure the highest possible specificity and sensitivity for each target gene. Reaction conditions for each of the reference and target genes are summarized in table 5, and qPCR programs used for final measurement can be found in table 6.

	Gene	cDNA dilution (final)	Primer concentration S (final)	Primer concentration AS (final)	Program
1	Actin β	1:500	0,5µM	0,5µM	+
		1:500	0,5µM	0,5µM	–
2	Gapdh	1:500	0,5µM	0,5µM	+
		1:500	0,5µM	0,5µM	–
3	Acly	1:500	0,5µM	0,5µM	+
4	Atp5h	1:500	0,5µM	0,5µM	+
5	Atg3	1:500	0,4µM	0,2µM	–
6	Cox5b	1:500	0,2µM	0,4µM	–
7	Cox7b	1:500	0,5µM	0,5µM	+ 5 additional cycles
8	Gabra2	1:500	0,5µM	0,5µM	+
9	Gabrg2	1:500	0,5µM	0,5µM	+
10	Gsr	1:500	0,5µM	0,5µM	+
11	Ndufa13	1:500	0,4µM	0,4µM	–
12	Nedd8	1:500	0,5µM	0,5µM	+
13	PGC-1α	1:500	1µM	1µM	–
14	Rheb	1:500	0,5µM	0,5µM	+
15	Sirt-1	1:500	0,5µM	0,5µM	+
16	Uba3	1:500	0,5µM	0,5µM	+

Table 5 Reaction conditions for gene expression measurement using qPCR S: sense primer, AS: antisense primer. + qPCR program run including extension time during the amplification step, - qPCR program run without extension time.

A. qPCR program run with extension time (+)

		Temperature (ºC)	Time		
Denaturation		95	15min		
Amplification	Denaturation	95	15s		45 cycles
	Annealing	60	20s		
	Extension	72	10s	Acquisition at end	
Melting curve analysis		65	1min	Continuous acquisition	
		95	Continuous	Continuous acquisition	
		37	1s		

B. qPCR program run without extension time (–)

		Temperature (ºC)	Time		
Denaturation		95	15min		
Amplification	Denaturation	95	15s		45 cycles
	Annealing	60	20s	Acquisition at end	
Melting curve analysis		65	1min	Continuous acquisition	
		95	Continuous	Continuous acquisition	
		37	1s		

Table 6 Thermal conditions for qPCR reactions. A. program run with extension time during the amplification step. B. program run under removal of extension time.

3.6. qPCR optimization

During the optimization of the qPCR setup, resulting in the final measurement conditions shown above, reaction conditions were modified repeatedly. This

concerns both reaction temperatures and times in qPCR programs as well as primer conditions.

In chapter 4.1., representative steps of the optimization process are presented for some of the genes of interest. For the purpose of qualitative analysis of PCR products, PCR was run on a BioRad C1000 Thermal Cycler (BioRad, Hercules, CA, USA). Except for modifications of primer concentrations, reagents and their concentrations were similar to the ones given above for qPCR. Conditions were as summarized in table 7. The conditions were kept similar to the amplification program of the qPCR conditions for expression analysis, as shown below.

		Temperature (°C)	Time	
Denaturation		95	15min	
Amplification	Denaturation	95	15s	35 - 40 cycles
	Annealing	60	20s	
	Extension	72	10s	

Table 7 Thermal conditions for PCR reactions for qualitative analysis of products under qPCR conditions.

Modification to this basic program needed for optimization are stated explicitly together with the respective results in chapter 4.1.

Amplification products of qualitative PCR and qPCR were run on 1% or 2% agarose gels in 0.5x TBE buffer (44.5mM Tris, 44.5mM Boric acid, 1.0mM EDTA, pH 8.0) containing SYBR Safe DNA gel stain (Invitrogen, Carlsbad, CA, USA) in 1:5,000 to 1:10,000 dilution.

Reaction products were diluted adequately for optimal visualization in dependence on the gene expression levels, and 6x DNA loading dye (Thermo Scientific, Waltham, MA, USA) was added prior to loading. 10µl of size standards (Quick-Load 50bp DNA Ladder or Quick-Load 100bp Ladder, New England Biolabs, Ipswich, MA, USA) were loaded in parallel. Gels were run at 60V for 60-120min and bands were visualized under UV light in an AlphaImager gel documentation system with AlphaImager Mini software (Protein Simple, Santa Clara, CA, USA).

3.7. Immunohistochemistry

Brains of 6 month-old wt and tg mice embedded in paraffin were prepared for immunohistochemistry (IHC). 5µm thick coronal sections were obtained (Microm HM240E, Thermo Scientific, Waltham, MA, USA), collected on microscope slides (Thermo Scientific, Waltham, MA, USA) and dried at 37°C over night. Hippocampal sections were collected from Bregma -4.30 to -6.50.

Sections were stained for endogenous PGC-1α, exogenous PGC-1α (represented by staining for flag-tag, i.e. DYKDDDDK tag), $GABA_A$ receptor subunit α2 (Gabra 2), and the neuronal nuclear antigen NeuN (Rbfox3 RNA binding protein, fox-1 homolog (C. elegans) 3) as a marker for neurons were performed. Antibodies and dilutions used are summarized in table 8.

Sections were deparaffinized in xylene two times for 5min each, followed by rehydration for two times 5min per step in a descending ethanol (99%, and 95%) to water series. For subsequent antigen retrieval, slides were heated in 0.01M citric acid solution at pH 6 (Sigma-Aldrich, Saint Louis, MO, USA) in a microwave oven three times for 5min intervals.

Following three short washing steps in PBS (137mM NaCl, 2.7mM KCl, 10mM $Na_2HPO_4 \bullet 2\ H_2O$, 2.0mM KH_2PO_4, pH 7.4), slides were incubated in 5% BSA in PBS-T (PBS supplemented with 0.1% v/v Triton X-100, Sigma Aldrich, Saint Louis, MO, USA) for 1h at RT for blocking. During the blocking step, antigen binding sides are saturated and as a consequence, binding of the antibodies to their target antigens is favored during the subsequent incubation in antibody solution. Primary antibodies diluted in 3% BSA in PBS-T and 3% BSA in PBS-T without added antibody for negative controls, respectively, were incubated with the tissue samples over night at 4°C in a humid chamber. Following two short rinsing steps in PBS-T, slides were washed in PBS-T three times for 5min. Secondary fluorochrome-coupled antibodies (summarized in table 8) diluted 1:500 in 3% BSA in PBS-T were incubated with the samples for 1h at room temperature.

For double stainings, slides were washed three times in PBS-T before repeating blocking, primary, and secondary antibody incubations for the respective second antibody as described above. Hoechst solution (bisBenzimide H 33258, Sigma Aldrich, Saint Louis, MO, USA), diluted to 0.4µg/ml in PBS, was applied as

counterstaining for nuclei. Before and following Hoechst-staining, slides were washed in PBS-T three times. Slides were mounted using Dabco mounting solution (Sigma Aldrich, Saint Louis, MO, USA). Images were acquired using a Leica DM 4500B fluorescence microscope (Leica Microsystems, Wetzlar, Germany).

Antibody	Reference number	Species	Clonality	Company	Dilution
Primary antibodies					
α- $GABA_A$ α2	AGA-002	rabbit	polyclonal	Alomone labs, Jerusalem, Israel	1:50
α- NeuN	MAB377	mouse	monoclonal	Merck Millipore, Billerica, MA, USA	1:300
α- PGC-1α	ST1202	mouse	monoclonal	Merck Millipore, Billerica, MA, USA	1:200
α- DYKDDDDK tag	2368	rabbit	polyclonal	Cell Signaling Technology, Inc., Danvers, MA, USA	1:100
Secondary antibodies (Alexa Fluor conjugated)					
α- mouse Alexa Fluor 594	A-21203	donkey	polyclonal	Invitrogen, Carlsbad, CA, USA	1:500
α- rabbit Alexa Fluor 488	A-21206	donkey	polyclonal	Invitrogen, Carlsbad, CA, USA	1:500

Table 8 Antibodies and dilutions for IHC.

4. Results

4.1. Optimization of the qPCR system

4.1.1. Confirmation of primer specificity

Prior to measurement of gene expression, reaction conditions were optimized for each of the reference and target genes. Since changes in expression levels in mature neurons are known to be relatively limited, it was important to ensure accurate quantification of mRNA levels in order to be able to detect possible small changes in gene expression levels. (Elstner et al. 2011)

As a first step, most of the primer pairs were found to bind specifically to their respective target genes and reliably mediate formation of specific products of the expected lengths in the qPCR reactions. However, for the target genes Atg3, Cox5b, Ndufa13, and PGC1α, an unspecific additional product was detected. Each of these additional products was found to be longer than the specific product, as shown in figure 6.

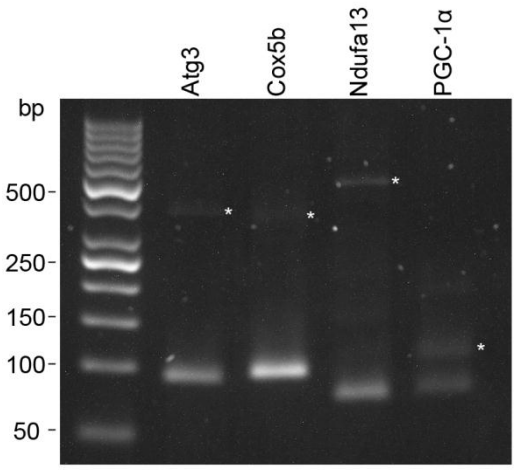

Figure 6 Agarose gel electrophoresis of qPCR products. qPCR products were run on a 1% agarose gel (100V, 75min). In addition to the respective specific products, reactions for each of the target genes produce additional, longer products (* unspecific products).

For the above mentioned target genes, reaction conditions had to be modified to eliminate formation of unspecific products. For these genes, the extension time (10s at 72°C) was removed from the amplification step of the qPCR reaction (see table 6). This renders the binding conditions for the primers more stringent. As a consequence, binding to the specific target sequence is favored over binding to unspecific sequences. In addition, different combinations of sense and antisense primer concentrations were tested for specificity of amplification product formation.

For the target genes Atg3, Cox5b, and Ndufa13, this approach resulted in sufficiently increased specificity for the targeted sequence to rule out formation of unspecific products, while maintaining reaction sensitivity.

For PGC-1α, however, an additional product slightly longer than the expected qPCR product was present even under modified conditions. Neither modification of the primer concentrations and their combinations nor adapting the annealing temperature resulted in formation of a single specific product. Representative gel images of PCR products formed under different reaction conditions are shown in figure 7a (modification of sense and antisense primer concentrations and their combination) and b (modification of the temperature during the annealing step of the amplification program).

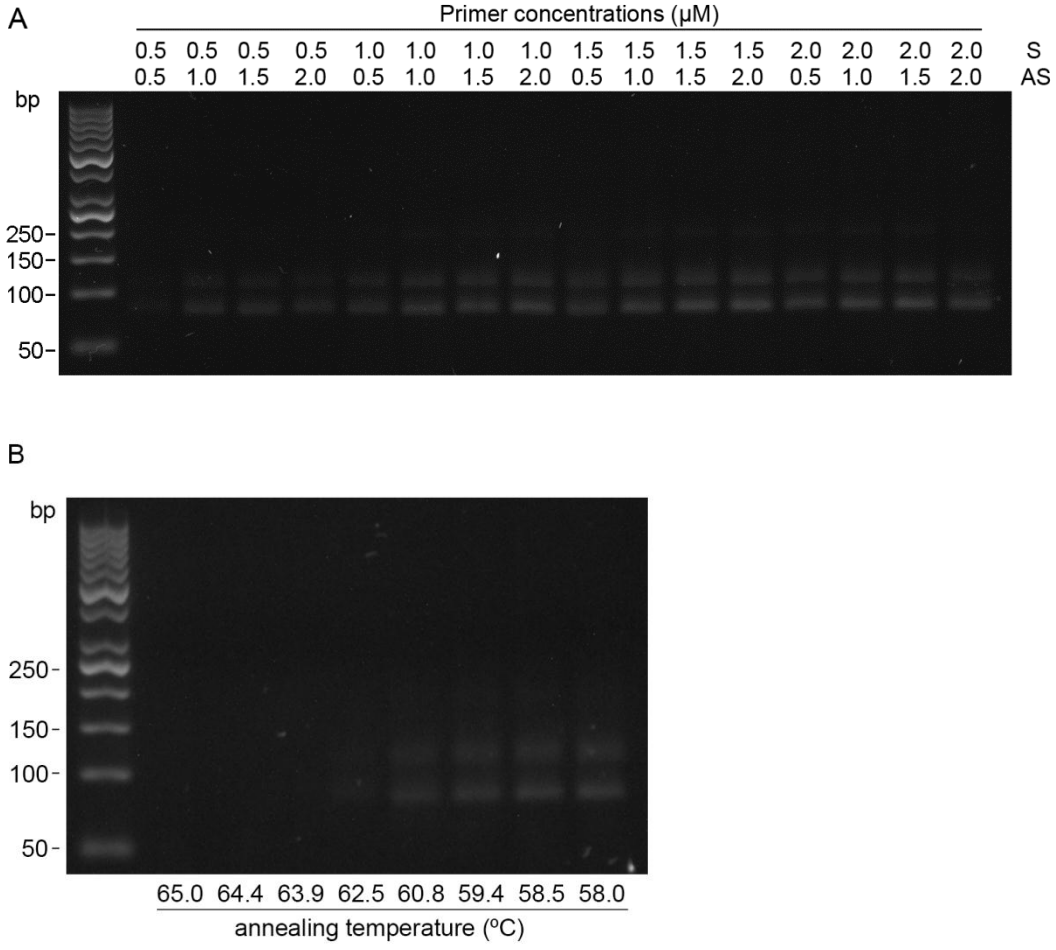

Figure 7 Modification of reaction conditions for PGC-1α. Formation of specific and unspecific amplification products was assessed qualitatively with agarose gel electrophoresis under modified reaction conditions. Shown are representative images of PCR products for hippocampal samples of wt controls. PCR products were run on 2% agarose gels (100V, 65min). PCR reaction conditions were as described in chapter 3, with modification of **A. Primer concentrations** (as given above) and **B. annealing temperatures** during the amplification step (as given above).

Blast search with the primer sequences (comparing to RefSeq RNA) revealed that the primer pairs for PGC-1α bind to two variants of the transcript of the PGC-1α gene (compare figure 8). The primers target transcript variant 1 (NCBI Reference Sequence: NM_008904.2), which encodes mRNA for PGC-1α. In addition, the primer pairs also recognize transcript variant 2 (NCBI Reference Sequence: NR_027710.1), which constitutes a non-coding mRNA.

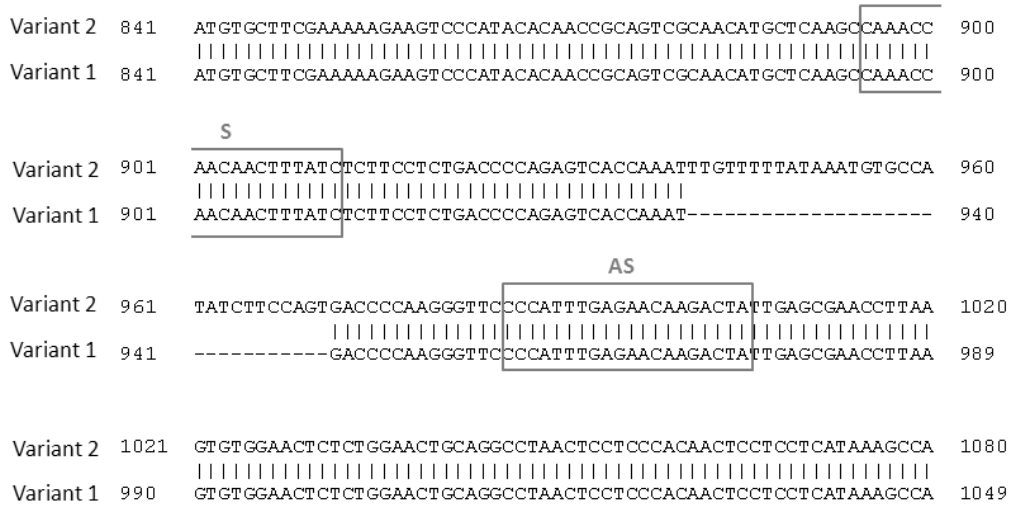

Figure 8 Blast sequence alignment of transcript variants of PGC-1α detected by the primers in use for qPCR. Blast sequence alignment to RefSeq RNA, variant 1: PGC-1α mRNA encoding transcript, variant 2: PGC-1α noncoding mRNA. Identities = 6464/6495 (99%), Gaps = 31/6495 (0%). Squares mark the region of primer binding (S: sense, AS: antisense).

The additional product thus most likely reflects a splice variant of the PGC-1α mRNA. The difference in sizes of the specific (80 bases) and additional product (~110 bases) as reflected by the bands detected in agarose gel electrophoresis (see figure 7), corresponds to the size of the additional region present in transcript variant 2. Except for this region, both splice variants have a similar nucleotide sequence and are both detected with equal sensitivity and specificity by the primers in use. For this reason, it was not possible to modify primer binding conditions in such a way as to favor binding to one transcript variant over the other.

The formation of an additional product in the qPCR reaction is also reflected in the melting temperature analysis. After the amplification reaction of the qPCR, a temperature gradient is applied while constantly measuring fluorescence intensity. The gradual increase ultimately causes products to dissipate at a temperature that reflects the binding affinity of both strands of the product. This melting point is

reflected by a steep decrease of fluorescence, since double stranded products dissipate into single stranded conformation. Apart from the melting temperature, the negative first derivative of the fluorescence intensity in dependence on the temperature is used to assess the specificity of product formation. Specific product formation commonly is reflected by a pronounced peak in the derivate. This corresponds to the temperature at which the decrease in fluorescence is steepest, and shows the dissipation of double stranded product. Additional peaks at lower temperatures reflect unspecific product formation, dissipating already at lower temperatures due to a lower binding affinity.

A representative melting curve for qPCR amplification of PGC-1α is shown in figure 9. The specific product (mRNA encoding transcript variant 1) has a melting temperature of 79.3ºC, whereas the product reflecting noncoding transcript variant 2 shows a decrease in fluorescence at a slightly lower temperature, having a melting temperature of 74.2 ºC.

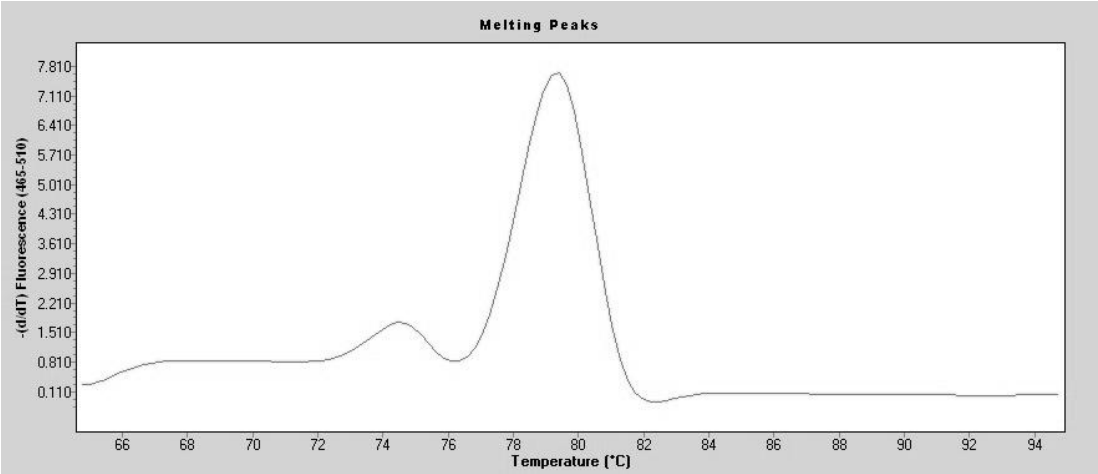

Figure 9 Melting curve analysis for PGC-1α. Melting analysis as performed with the LightCycler analysis software (Roche Diagnostics, Basel, Switzerland). The figure shows a representative image of a melting curve for qPCR amplification for PGC-1α (reaction conditions were as described in chapter 3).

Transgene expression exclusively results in formation of coding variant 1, since the exogenous PGC-1α gene was inserted in form of cDNA reflecting only the protein-coding transcript. Considering the fact that the additional product reflects a transcript variant of the endogenous PGC-1α gene encoding a non-coding mRNA, it is conceivable that the formation of this product does not interfere with a reliable detection of the gene expression levels. mRNA levels measured for PGC-1α comprise both the endogenous as well as the expression of the transgene.

Formation of a qPCR product specific for the target genes was assessed from the melting curves for each primer pair as well as by agarose gel electrophoresis of the qPCR products. This allows comparing the lengths of the products to the expected length of the amplified sequences and excluding the formation of additional, unspecific products. Amplification products of qPCR reactions for each of the reference and target genes in hippocampal and cortical samples of both wt and tg animals were run on agarose gels, as shown by representative gel images in figure 10. Products of the qPCR reactions for reference genes actin β and GAPDH were formed in a similar way in both qPCR amplification programs in use. No differences could be observed between samples from PGC-1α tg and control mice.

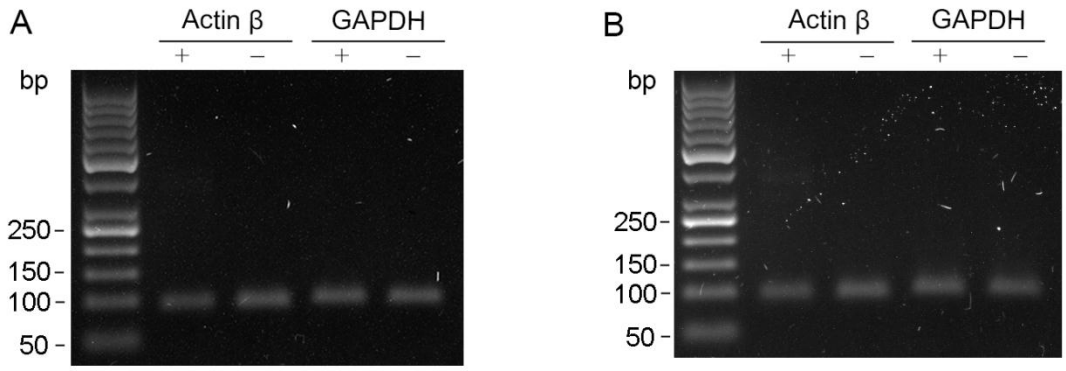

Figure 10 Formation of specific amplification products for reference genes. qPCR amplification products for Actin β and GAPDH were run on agarose gels (2%, 60V, 60min). Shown are representative images for hippocampal sample. **A. wt control B. PGC-1α tg.** + qPCR program with extension time included in the amplification step, - qPCR program without extension time.

Likewise, qPCR products for the target genes produced under the conditions used for gene expression measurements were analyzed electrophoretically. Figure 11 depicts a typical gel image.

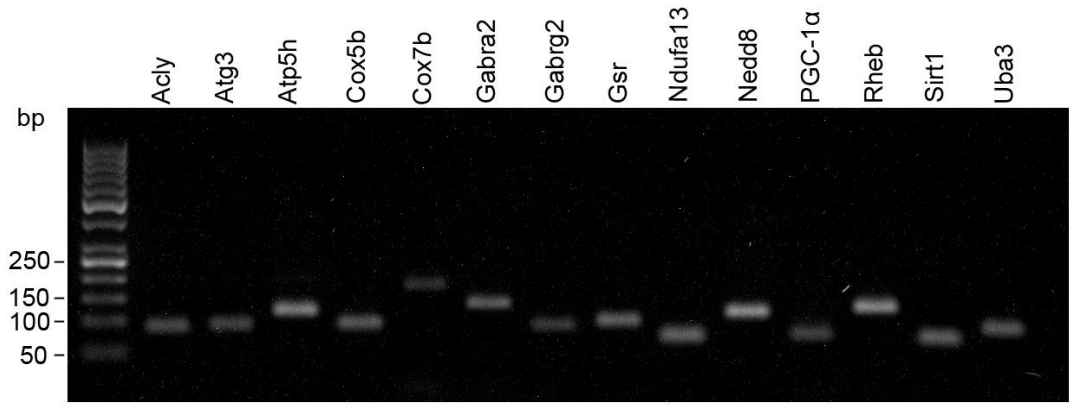

Figure 11 Formation of specific amplification products for target genes. qPCR amplification products for target genes were run on agarose gels (2%, 60V, 100min; for qPCR reaction conditions, see chapter 3). qPCR products were diluted to ensure optimal visualization) . Given here is a representative image for product analysis (Hc of PGC-1α tg mouse).

A double band for PGC-1α could be observed in some qPCR reactions, but was not detectable throughout all gel images taken. Presumably, this is due to a higher relative amount of the specific product observed for the tg mice. As for the remaining target genes, formation of a single product was shown for PGC-1α tg and wt mice. Lengths of qPCR product were matching the expected qPCR products for the reference and target genes, as summarized in table 9.

Gene	Expected length of the product (bases)
Actin β	95
GAPDH	101
Acly	91
Atg3	93
Atp5h	128
Cox5b	98
Cox7b	185
Gabra2	149
Gabrg2	99
Gsr	108
Ndufa13	77
Nedd8	128
PGC-1α	80
Rheb	138
Sirt-1	74
Uba3	93

Table 9 Expected lengths of amplification products in qPCR.

4.1.2. Efficiency measurements

Efficiencies of the qPCR reactions of the reference genes were assessed to ensure a comparable level of amplification efficiencies among samples from both control and tg mice for both reference genes. Efficiencies were measured in hippocampal mRNA samples. Preceding tests were performed to ensure comparability between Hc and Cx. Since these test measurements yielded highly similar results for both tissues, efficiency measurements were done using hippocampal mRNA. The efficiencies derived from these measurements were used for gene expression measurements in hippocampal and cortical samples.

Efficiency calculations were based on cDNA input dilution series spanning several orders of magnitude. Cp values corresponding to the dilution steps are plotted against the decadic logarithm of the respective dilutions of cDNA input. Linear regression upon the measured data points yields a linear graph, from whose slope the reaction efficiency can be calculated. The relationship between efficiency and the slope of the regression line is given as follows, *adapted from* (Dorak 2006):

$$\frac{\Delta y}{\Delta x} = -\frac{1}{log_{10}(eff)}$$

In the equation, (eff) corresponds to the efficiency and $\frac{\Delta y}{\Delta x}$ represents the slope. If a perfect doubling of template occurs during each cycle, the efficiency value equals 2.0. In this case, the slope of the regression line is -3.32. The efficiency of the qPCR reaction corresponds to the rate of amplification. In case the efficiencies are exceedingly higher or lower, the reaction conditions most likely are not suitable for ensuring a reliable amplification and detection. (VanGuilder, Vrana & Freeman 2008, Dorak 2006)

Efficiencies vary in dependence on the length of the qPCR product and the base composition, among other factors. One of the main influencers of efficiency is the cDNA concentration in the starting reaction. For this reason, the dynamic range is an important parameter for qPCR performance. This range corresponds to the cDNA concentrations that can be used as input and result in comparable and reliable qPCR reactions.

qPCR was performed using cDNA concentrations spanning four orders of magnitude as input in order to assess the dynamic range of the qPCR reactions. Reaction

effiencies were calculated from a linear regression analysis based on the Cp values obtained for a number of cDNA dilutions within the above mentioned range.

For reference genes, this resulted in efficiencies ranging from 1.95 to 2.07. These values are very close to the ideal reaction, which would correspond to 2.00, and the amplification reactions can be considered to yield highly reliable results over the dynamic range of four orders of magnitude. Slightly different patterns were observed for the amplification of GAPDH from mRNA of tg mice under amplification conditions including an extension step. Here, a higher efficiency (2.22) was observed. Especially in view with the high reliability of the remaining reactions, this value as determined to lie within the acceptable range.

Gene		Efficiency	Slope
+ (with extension time)			
Actin β	control	1,96	-3,419
	PGC-1α tg	2,05	-3,213
GAPDH	control	1,97	-3,407
	PGC-1α tg	2,22	-2,884
− (without extension time)			
Actin β	control	1,98	-3,38
	PGC-1α tg	2,07	-3,158
GAPDH	control	1,95	-3,459
	PGC-1α tg	1,98	-3,369

Table 10 Efficiencies of qPCR reactions for reference genes.

Figure 12 shows the efficiency curves for both reference genes for wt and PGC-1α tg mice under both measurement conditions in use. Regression lines of Cp values plotted against the range of cDNA dilutions used to determine the reaction efficiencies are depicted.

The efficiencies for reference genes can be considered to have comparable levels among wt control and PGC-1α tg mice as well as in both qPCR programs used (for a summary of reaction conditions and program setup see chapter 3).

For measurements of gene expression levels, a final cDNA dilution of 1:500 in the reactions (indicated in the graphs by arrows) was used for all of the target genes. This cDNA concentration lies well within the linear range of the qPCR assay. As shown in figure 12, this cDNA dilution is within the range in which all of the efficiency functions lie close together within a very narrow range.

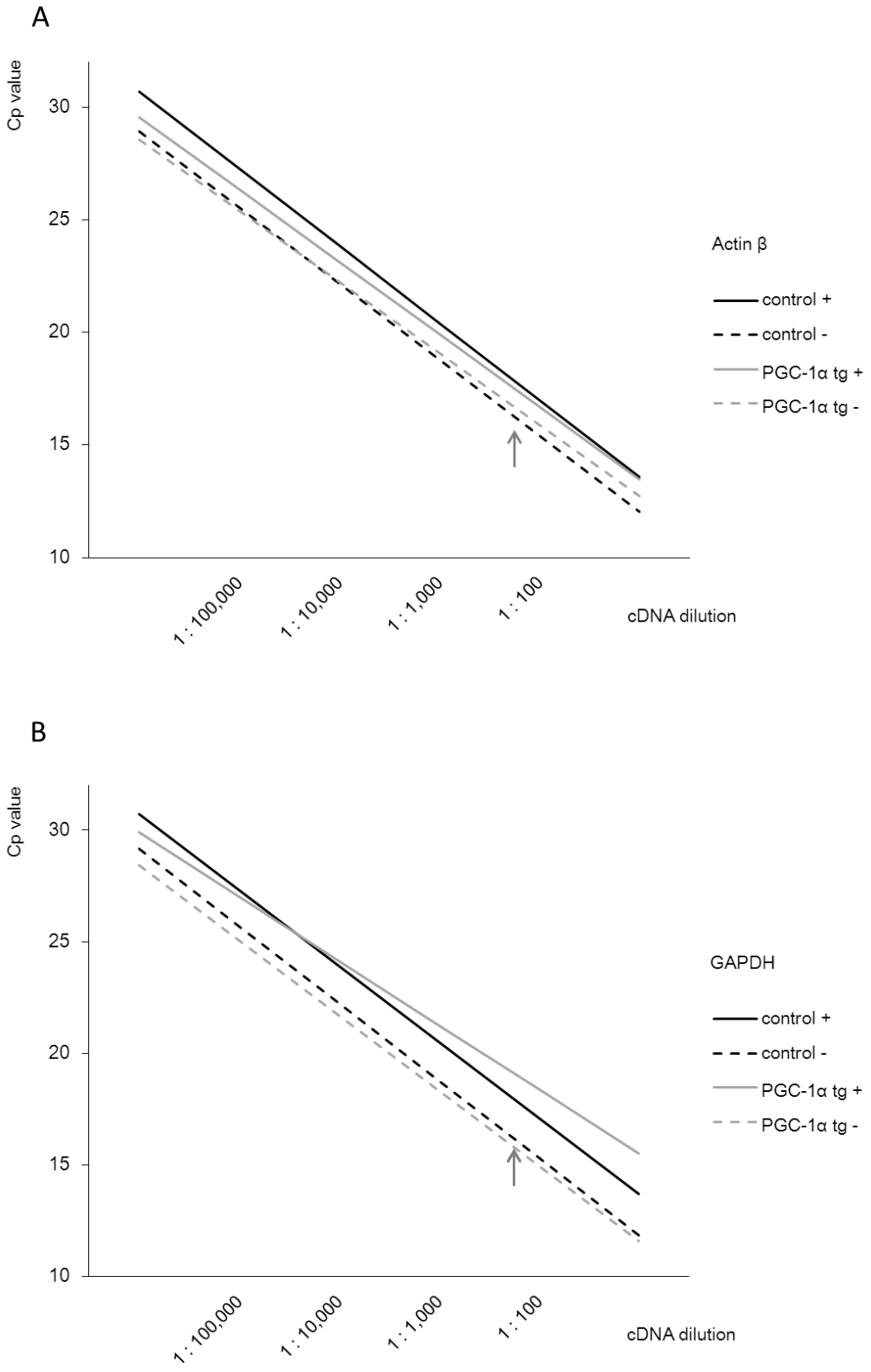

Figure 12 Efficiencies of qPCR reactions for reference genes. Shown are regression curves for efficiencies of reference genes **A. Actin β** and **B. GAPDH**. + qPCR program run with extension time during the amplification, - qPCR program without extension time.

qPCR products were run on agarose gels to assess reaction specificity as described in chapter 3. Reactions with cDNA dilutions spanning four orders of magnitude as input were shown to produce specific products at the expected lengths for both reference genes. This held true for control and PGC-1α tg mice. Equally, removing the extension step from the amplification reaction of the qPCR program did not interfere with the specific formation of products.

Similar to the approach used for the reference genes, reaction efficiencies were tested for all genes of interest over a range of two to four orders of magnitude. Dilution ranges and measurement points were chosen in dependence on theoretical estimations of expression levels and preceding qPCR test runs. Reaction conditions can be found in chapter 3. Efficiencies are summarized below in table 11:

Gene	qPCR program	efficiency	slope
Acly	+	1.93	-3.512
Atg3	+	1.92	-3.519
Atp5h	–	2.00	-3.331
Cox5b	–	1.92	-3.525
Cox7b	+	2.15	-3.017
Gabra2	+	2.05	-3.209
Gabrg2	+	1.90	-3.579
Gsr	+	1.90	-3.580
Ndufa13	–	1.91	-3.572
Nedd8	+	1.76	-4.059
PGC-1α	–	2.07	-3.170
Rheb	+	1.85	-3.732
Sirt-1	+	1.97	-3.408
Uba3	+	1.96	-3.431

Table 11 Efficiencies of qPCR reactions for target genes. + qPCR program run including extension time during the amplification step, - qPCR program run without extension time.

The efficiencies given here have been measured using hippocampal RNA of wt mice. Test measurements comparing hippocampal and cortical expression of the target genes in both wt as well as tg mice were performed to ensure comparability.

In consideration of the parameters determined in the optimization process described above, final conditions for measurements of gene expression were chosen (as described in chapter 3.).

Efficiencies were taken into account for calculation of relative expression levels. Calculations were based on the ΔΔCp method, as reviewed in chapter 1.5.

4.2. Gene expression analysis

4.2.1. Expression analysis of PGC-1α

The initial study characterizing the PGC-1α tg mouse line revealed a strong increase in PGC-1α protein levels in SNc of tg mice. Exogenous PGC-1α was strongly expressed throughout the studied brain regions. (Mudo et al. 2012) Equally, a microarray based screening (GeneChip Mouse Exon ST Array, Affymetrix, Santa Clara, CA, USA), showed increased expression of PGC-1α in Hc and Cx of tg mice.

In order to further characterize gene expression patterns in PGC-1α tg mice, we assessed expression levels of PGC-1α mRNA. This includes expression of both the endogenous gene as well as expression driven by the transgene.

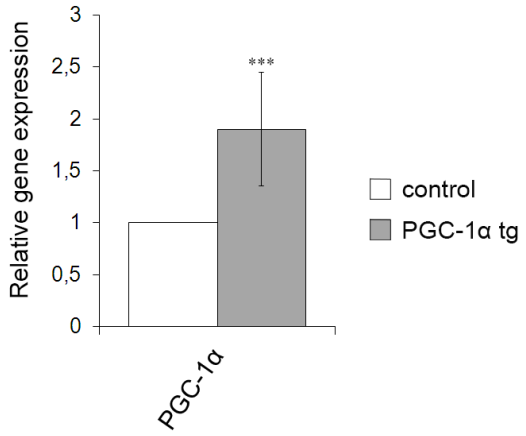

Figure 13 Gene expression analysis for PGC-1α in Hc. Relative expression levels in Hc of PGC-1α tg mice, ± standard deviation (stdev). Stars denote statistical significance compared to wt controls (*** p<0.001).

As expected, PGC-1α expression is increased in Hc of tg mice. The average increase amounts to 1.90 ± 0.55. This expression value is, as all of the following values, given as average expression among the PGC-1α tg mice in comparison to wt controls (set to 1.00). Errors are denoted as standard deviation (stdev).

The high standard deviation can be attributed to individual differences in gene expression levels that were found among the PGC-1α tg mice.

PGC-1α mRNA expression levels in cortical samples of tg mice paralleled the findings in Hc, with a pronounced increase in the expression levels of PGC-1α being detected. The expression levels are slightly lower than in Hc, averaging to 1.79 ± 0.45 as compared to wt mice.

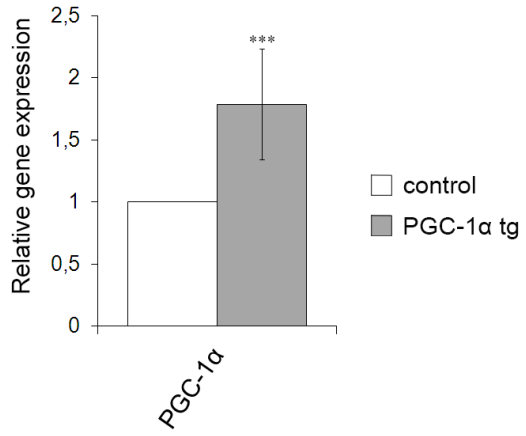

Figure 14 Gene expression analysis for PGC-1α in Cx. Relative expression levels in Cx of PGC-1α tg mice, ± stdev. Stars denote statistical significance compared to wt controls (*** p<0.001).

Next, we sought to determine immunohistochemically whether the increase in PGC-1α mRNA levels entails higher protein levels.

Endogenous PGC-1α expression in the brains of wt mice has been characterized previously. (Tritos et al. 2003) The characterization was done for the strain that constitutes the wt controls and genetic background of tg mice for this study. In line with the findings reported by Tritos and collegues, widespread expression of PGC-1α in Hc of wt controls was observed. (Tritos et al. 2003) Immunostaining for PGC-1α targets both endogenous as well as the transgenic protein, and the overall expression pattern did not appear to differ between wt controls and PGC-1α tg mice.

As the expression levels measured by qPCR comprise both the endogenous as well as the transgene driven mRNA expression for PGC-1α, we sought to verify the presence of exogenous PGC-1α in the tg mice.

Exogenous PGC-1α protein is expressed with a flag-tag, and can therefore be distinguished immunohistochemically from the endogenously expressed PGC-1α. (Mudo et al. 2012) Simultaneous immunohistochemical detection of NeuN as a neuronal maker and flag-tag, marking exogenous PGC-1α, was performed in order to study the expression pattern of transgenic PGC-1α in hippocampal and cortical neurons. Representative images are shown in figure 15.

Immunohistochemical staining for flag-tag revealed a widespread expression of exogenous PGC-1α in hippocampal and cortical neurons of PGC-1α tg mice, as shown by colocalization of NeuN and flag-tagged PGC-1α. In contrast, no signal for flag-tag could be detected in the wt controls.

Furthermore, immunostainings for PGC-1α and flag-tag were performed. In accordance with the results presented above, signals for PGC-1α and flag were colocalized to the same cells throughout the Hc and Cx of PGC-1α tg mice, as shown by representative images in figure 16.

An interesting aspect of transgene driven PGC-1α expression that was revealed by immunostainings is the subcellular expression pattern. Whereas PGC-1α staining was located mostly to the nuclei of neurons, flag-tag positive PGC-1α staining rather appeared to accumulate in close proximity to, but outside of the nucleus.

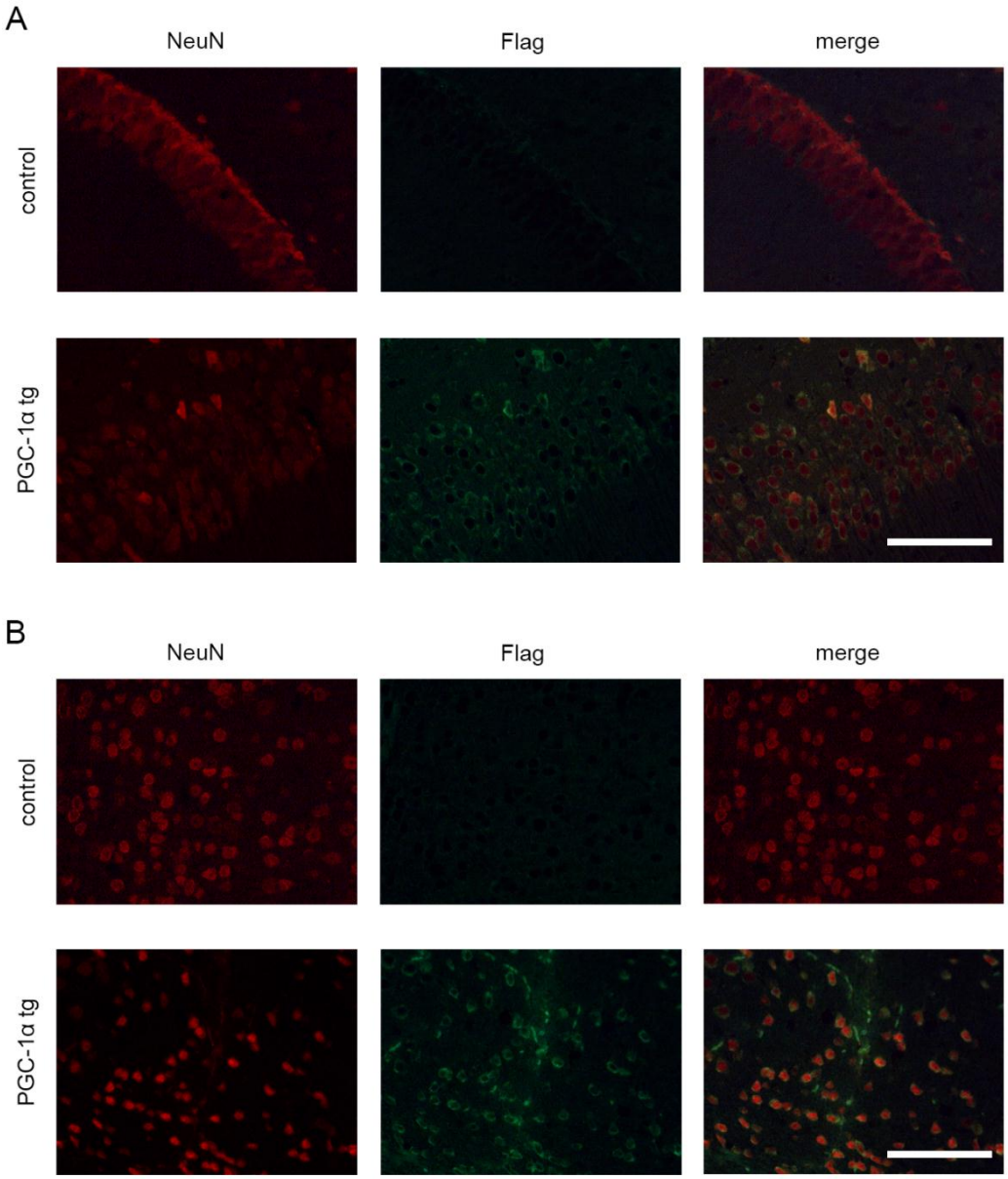

Figure 15 Colocalization analysis for NeuN and flag-tagged exogenous PGC-1α. Immunostainings for the neuronal marker NeuN and flag-tag as a surrogate marker for exogenous PGC-1α in **A. Hc** and **B. Cx**. Upper panels (control): wt controls, lower panels (PGC-1α tg): PGC-1α tg mice. 20x magnification, scale bar 100μm.

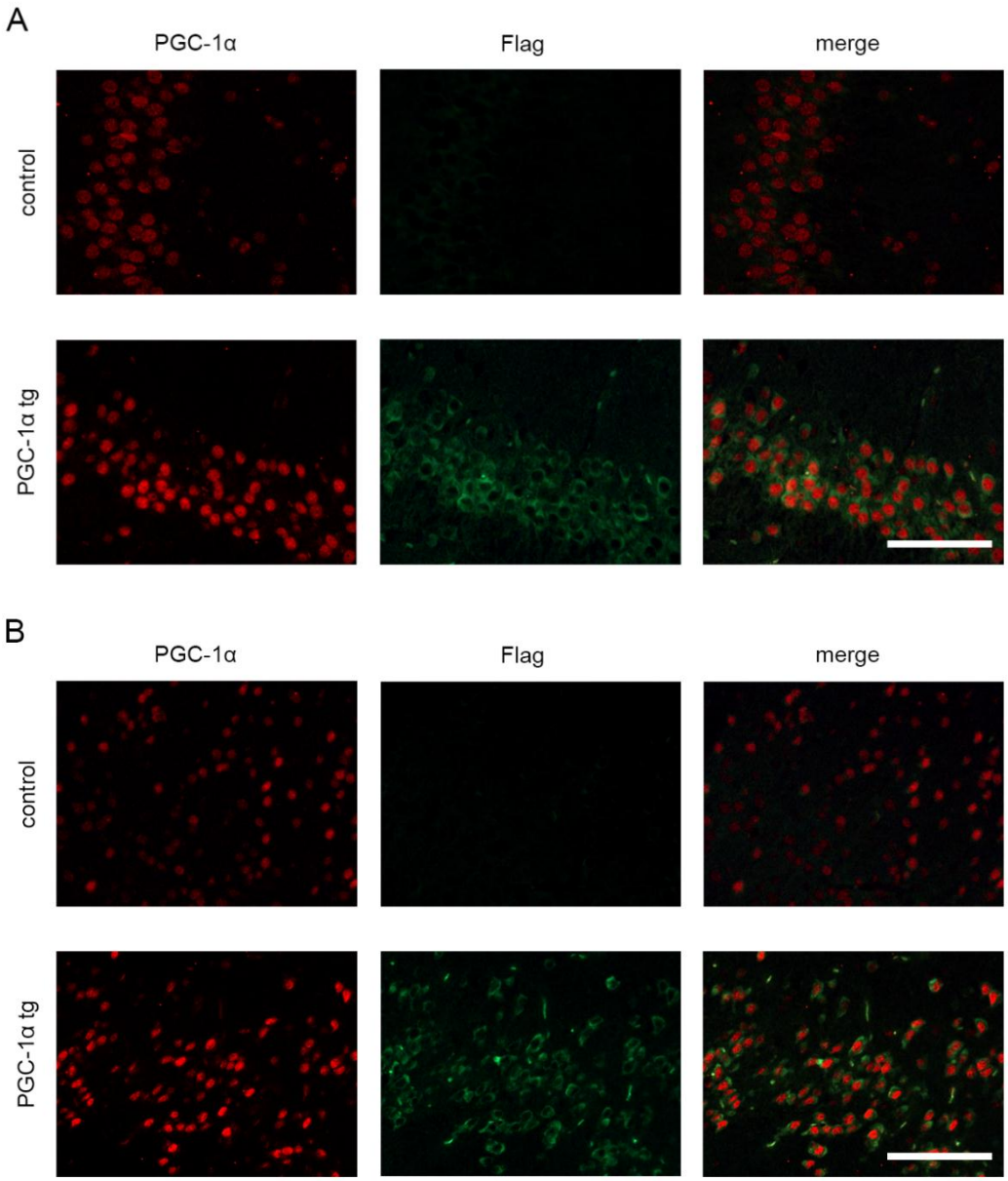

Figure 16 Colocalization analysis for PGC-1α and flag-tagged exogenous PGC-1α. Immunostainings for PGC-1α and flag-tag as a surrogate marker for exogenous PGC-1α in **A. Hc** and **B. Cx**. Upper panels (control): wt controls, lower panels (PGC-1α tg): PGC-1α tg mice. 20x magnification, scale bar 100μm.

These findings show that transgenic introduction of the PGC-1α gene causes flag-tagged exogenous PGC-1α to be expressed in hippocampal and cortical neurons in the PGC-1α tg mouse line. This is in line with the characterization studies of transgene expression in substantia nigra reported by Mudò et al. (Mudo et al. 2012)

Pronounced increases in mRNA levels of PGC-1α parallel the presence of exogenous PGC-1α in neurons in both tissues studied in this Master's thesis study. Insertion of the transgene causes increases in the transcription of PGC-1α, with the mRNA population reflecting expression of both endogenous as well as exogenous PGC-1α. The enhanced mRNA transcription can therefore at least partly be attributed to expression of the transgene.

Mudò et al showed that the PGC-1α transgene expression entails increased protein levels in substantia nigra. Taking this into account, the above described findings suggest that the increase in transcriptional activity likely is reflected by higher amounts of PGC-1α on the protein level in Hc and Cx. (Mudo et al. 2012)

Similarly and expectedly, the transgene expression is reflected by the presence of flag-tagged PGC-1α in neurons. Therefore, changes in gene expression levels can most likely be attributed to neurons.

A surprising observation in hippocampal and cortical sections of tg mice were the presence of strongly PGC-1α and flag positive extranuclear signals taking on elongated forms. This, translation into protein and PGC-1α activity levels under transgene expression remain to be studied.

PGC-1α activity is known to be directly regulated by the deacetylase Sirt-1. (Canto, Auwerx 2009) We hypothesized that PGC-1α overexpression might have an influence on gene expression of Sirt-1 via possible feedback loops. The expression levels of Sirt-1 in Hc were therefore measured.

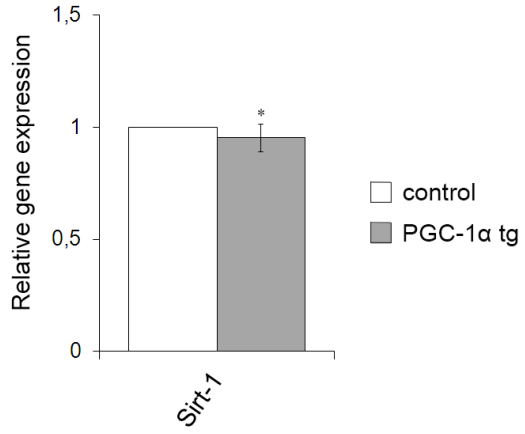

Figure 17 Gene expression analysis for Sirt-1 in Hc. Relative expression levels in Hc of PGC-1α tg mice, ± stdev. Stars denote statistical significance compared to wt controls (* p<0.05).

Sirt-1 1 mRNA levels showed a small, but significant decrease in Hc of tg mice. mRNA expression was 0.95 ± 0.06 in tg mice as compared to wt controls.

4.2.2. Partial downregulation of mitochondrial metabolic enzymes

Given that PGC-1α is a known master regulator of mitochondrial metabolism, and obtains an essential function to maintain energetic homeostasis in neurons, we asked whether PGC-1α overexpression has a long-term impact on mitochondrial oxidative phosphorylation. (Kelly, Scarpulla 2004, Puigserver, Spiegelman 2003, Wareski et al. 2009) We hypothesized that PGC-1α overexpression might entail sustained changes in metabolic activity in the brains of tg mice that are attributable to transcriptional regulation.

In order to encompass possible gene expression changes along oxidative metabolism pathways, we chose a number of genes encoding for enzymes catalyzing reactions at different stages of metabolism. *Reviewed in* (Duchen 2004, Nunnari, Suomalainen 2012, Abou-Sleiman, Muqit & Wood 2006)

These included, firstly, citrate lyase (Acly), the enzyme producing acetyl-CoA by cleavage of citrate. The enzyme itself is located in the cytosol, but its substrate and product are produced and metabolized, respectively, in mitochondria. Acetyl-CoA provides the link between glucose and fatty acid metabolic pathways, and is integral part of cellular respiration. It enters the citric acid cycle, which in turn yields the

electron carriers NADH and $FADH_2$ fuelling the mitochondrial electron transport chain. (Chypre, Zaidi & Smans 2012)

Furthermore, genes encoding respiratory chain subunits were chosen:

NADH dehydrogenase 1α is the entry enzyme for electrons transferred by NADH into the respiratory chain. (Duchen 2004) Disturbances in complex I functionality have been linked to neurodegeneration and are strongly implicated in PD pathogenesis. (Winklhofer, Haass 2010) The complex I inhibitor MPTP is used as a means to induce parkinsonism in animal models. (Przedborski et al. 2004) Furthermore, PGC-1α overexpression is protective against MPTP treatment in tg mice. (Mudo et al. 2012) As a representative subunit of this complex, subunit 13 (Ndufa13) was chosen for gene expression studies.

Complex IV, cytochrome c oxidase, has been implicated in oxidative stress generation. (Srinivasan, Avadhani 2012) Hypothesizing that PGC-1α mediated neuroprotection might involve changes in expression of ETC complexes, we chose to include two subunits of complex IV, cytochrome c oxidase into our studies. Here, gene expression of subunits Vb (Cox5b) and VIIb (Cox7b) was measured.

Since PGC-1α tg mice showed an increased respiratory control, the site of actual ATP production, F_1F_O ATP synthase, was of interest. (Duchen 2004, Mudo et al. 2012) Gene expression was measured for ATP synthase, H^+ transporting, mitochondrial F_o complex, subunit d (Atp5h).

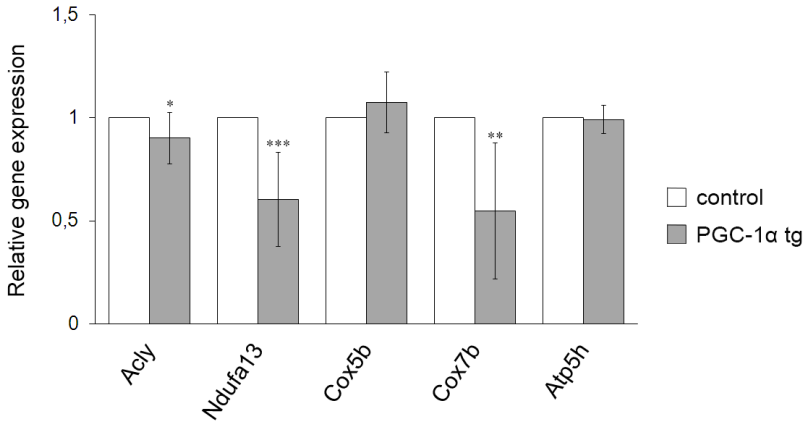

Figure 18 Gene expression analysis of enzymes involved in mitochondrial energy metabolism in Hc. Relative expression levels in Hc of PGC-1α tg mice, ± stdev. Stars denote statistical significance compared to wt controls (* p<0.05, ** p<0.01, *** p<0.001).

Strikingly, gene expression levels of all of the above named enzymes involved in energy metabolism were found to be either reduced or unchanged in Hc of PGC-1α tg mice.

Acly was found to be slightly, but significantly downregulated (0.90 ± 0.12). A more pronounced underexpression was found for Ndfua13, averaging at 0.64 ± 0.23.

No differences between PGC-1α tg and wt mice could be detected in the expression of Cox5b. In contrast to the latter finding, mRNA for Cox7b was strongly underexpressed in PGC-1α tg mice, at an average of 0.55 ± 0.33 of control expression.

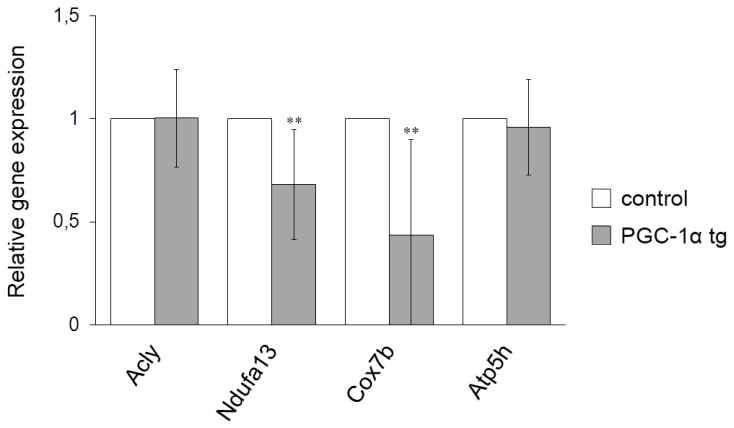

Figure 19 Gene expression analysis of enzymes involved in mitochondrial energy metabolism in Cx. Relative expression levels in Cx of PGC-1α tg mice, ± stdev. Stars denote statistical significance compared to wt controls (** p<0.01).

Similar to the findings in hippocampal tissue, gene expression of respiratory chain enzyme subunits was either unchanged or decreased in cortical samples. Here, no difference could be measured in mRNA levels reflecting citrate lyase expression. Equally, and similarly to the findings in hippocampal RNA extracts, Atp5h expression was unaffected by PGC-1α overexpression.

However, in a strong similarity to the findings in Hc, also Cx of PGC-1 α tg mice showed strong underexpression of Ndufa13 (0.68 ± 0.27) and Cox7b (0.44 ± 0.46).

The small decrease of Acly expression in Hc, as well as the unchanged expression in Cx were paralleling the microarray based results. Similarly, Cox7b underexpression had been indicated by microarray results for Hc, but not Cx.

Cox5b, Ndufa13, and Atp5h had been indicated to be slightly upregulated by the microarray. These values could not be confirmed with the qPCR based measurements.

4.2.3. Upregulation of the mitochondrial antioxidant system

Representative of the mitochondrial antioxidant system known to be under the regulation of PGC-1α, expression levels of glutathione reductase (Gsr) were measured. (Nicholls 2002)

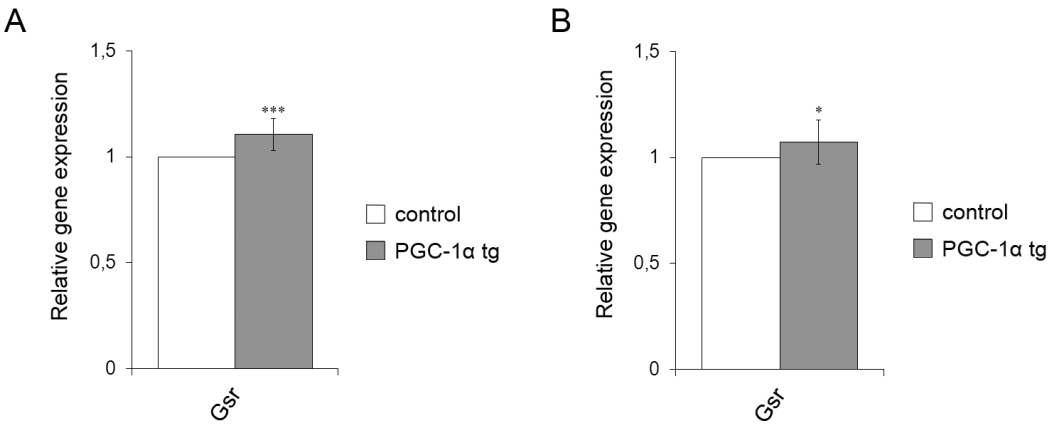

Figure 20 Gene expression analysis for Gsr. Relative expression levels of Gsr in **A. Hc** and **B. Cx** of PGC-1α tg mice, ± stdev; stars denote statistical significance compared to wt controls (* p<0.05, *** p<0.001).

Similar small but significant increases in the expression level in Hc (1.11, Stdev 0.08) as well as Cx (1.07, Stdev 0.10) of tg mice were observed. These findings parallel the upregulation found with the microarray based study, even though these screening results indicated a higher increase in gene expression.

4.2.4. Expression analysis of nonmitochondrial pathways implied in Parkinson's Disease

In order to assess influences of PGC-1α overexpression on pathways involved in the regulation of neuronal survival by growth factors and nutrient sensing networks, we measured mRNA levels of the Ras-family member protein Ras homolog enriched in brain (Rheb). Rheb is part of the mTOR signaling pathway and known to be underexpressed in DA neurons in PD. (Lee, Giordano & Zhang 2012, Elstner et al. 2011)

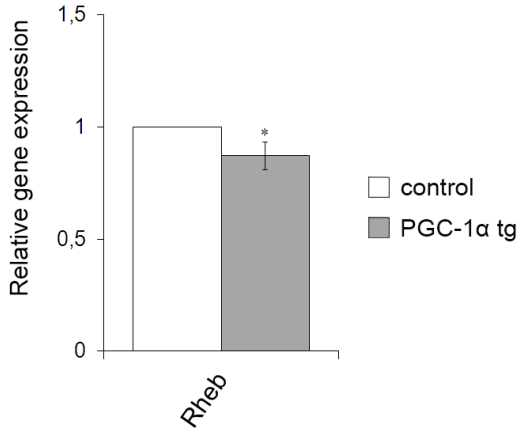

Figure 21 Gene expression analysis for Rheb in Hc. Relative expression levels of Rheb in Hc of PGC-1α tg mice, ± stdev. Stars denote statistical significance compared to wt controls (* p<0.05).

In Hc samples of tg mice, Rheb was somewhat underexpressed (0.87 ± 0.15) in comparison to wt mice, confirming values measured by microarray.

mTOR signaling is involved in the regulation of autophagy. Due to the known role of protein scavenging and degradation in PD pathogenesis, we were interested in possible changes of regulatory protein modifications under PGC-1α overexpression. (Kim, Rodriguez-Enriquez & Lemasters 2007, Lee, Giordano & Zhang 2012)

Expression levels of autophagocytosis associated protein 3 (Atg3) were measured in Hc of tg mice. Atg3 has a role in mediating autophagocytotic degradation of organelles, and is a ubiquitin-like modifier. (Lee, Giordano & Zhang 2012)

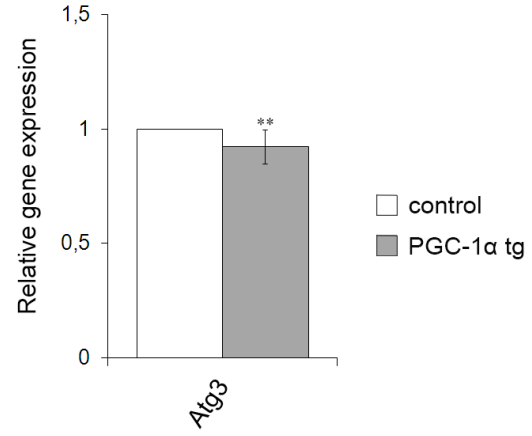

Figure 22 Gene expression analysis for Atg3 in Hc. Relative expression levels of Atg3 in Hc of PGC-1α tg mice, ± stdev. Stars denote statistical significance compared to wt controls (** p<0.01).

With average expression levels of 0.92 ± 0.07 in PGC-1α tg mice, Atg3 showed a small, but significant underexpression.

Ubiquitin-like modifier activating enzyme 3 (Uba3) mediates activation of Neural precursor cell expressed, developmentally down-regulated 8 (Nedd8). This pathway, among others, influences cell cycle progression. (Gong, Yeh 1999, Kamitani et al. 1997)

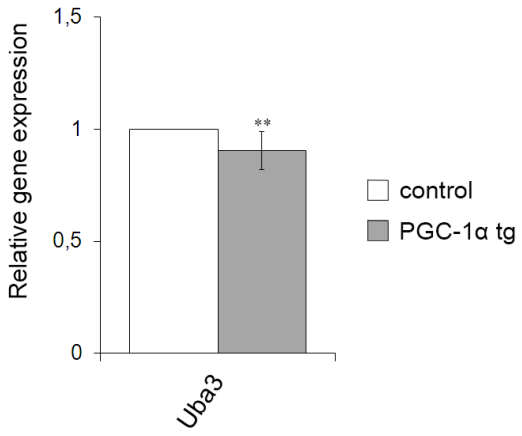

Figure 23 Gene expression analysis for Uba3 in Hc. Relative expression levels of Uba3 in Hc of PGC-1α tg mice, ± stdev. Stars denote statistical significance compared to wt controls (** p<0.01).

In Hc of PGC-1α tg mice, Uba3 expression was slightly reduced (0.90 ± 0.08).

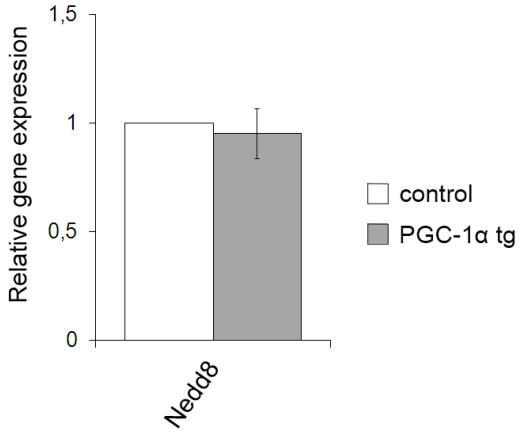

Figure 24 Gene expression analysis for Nedd8 in Hc. Relative expression levels of Nedd8 in Hc of PGC-1α tg mice, ± stdev.

Nedd8 mRNA levels in Hc showed no detectable differences between PGC-1α tg and wt mice.

The expression values for Atg3, Uba3, and Nedd8 are somewhat contradictory to a slight upregulation indicated by the microarray.

4.2.5. Differential expression of $GABA_A$ receptor subunits

The microarray based screening revealed a pronounced upregulation of subunit α2 of the $GABA_A$ receptor. In accordance with reports about involvement of PGC-1α in the regulation of survival of GABAergic neurons in rat brain and differential regulation of $GABA_A$ receptor subunits in neurodegenerative diseases, PGC-1α overexpression seemed to be altering the expression of at least two subunits. (Cowell, Blake & Russell 2007, Luchetti, Huitinga & Swaab 2011) For this reason, we sought to verify the differential regulation for $GABA_A$ receptor subunits α2 (Gabra2) and γ2 (Gabrg2).

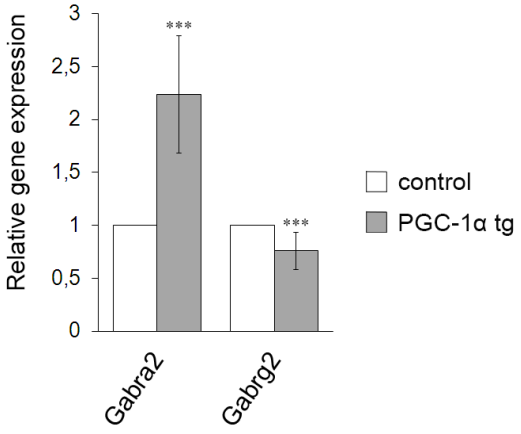

Figure 25 Gene expression analysis for Gabra2 and Gabrg2 in Hc. Relative expression levels in Hc of PGC-1α tg mice, ± stdev. Stars denote statistical significance compared to wt controls (*** p<0.001).

In line with the microarray results, indicative of an approximately 2.5 fold increase compared to wt controls, Gabra2 was found to be highly upregulated in Hc of PGC-1α tg mice. The average expression level in comparison to wt controls was 2.24 ± 0.55.

In contrast, the upregulation could not be verified for Gabrg2. Expression was found to be decreased in a highly significant manner to 0.76 ± 0.18 in comparison to wt controls, whereas the microarray results had pointed towards a slight upregulation (in the screening, an expression value of 1.21 in tg mice was reported).

These findings suggest a strong relative shift in the subunit composition of $GABA_A$ receptors, with an increased number α2 containing receptors present in brains of tg mice. To further characterize the strong upregulation of $GABA_A$ receptor subunit α2 expression, we sought to determine expression patterns in Hc immunohistochemically. Representative images for colocalization studies of Gabra2 with NeuN and PGC-1α, respectively, are shown in figure 26.

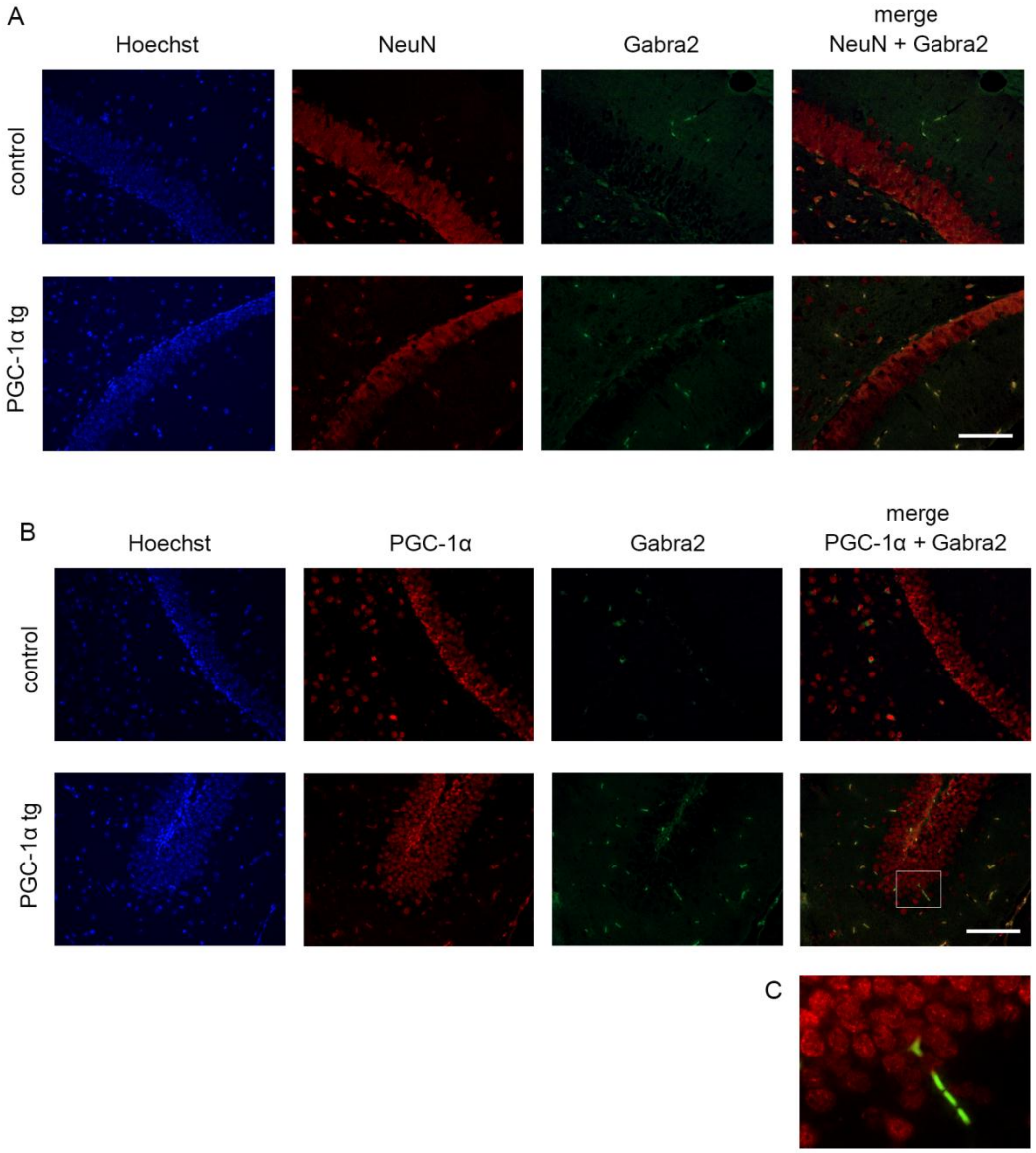

Figure 26 Localization analysis for Gabra2 in Hc. A. Colocalization analysis for NeuN and Gabra2. Immunostainings for the neuronal marker NeuN and Gabra2. **B. Colocalization analysis for PGC-1α and Gabra2.** Immunostainings for PGC-1α and Gabra2. Upper panels (control): wt controls, lower panels (PGC-1α tg): PGC-1α tg mice. A. and B. 20x magnification, C. 100x magnification, scale bar 100μm. **C. Subcellular localization of Gabra2.** Magnification of the area marked in B.

Gabra2 was found to be expressed throughout the Hc of both wt and PGC-1α tg mice. Expression appeared to be restricted to neuronal nuclei, as shown in figure 26 A by colocalization of the neuronal nuclear antigen NeuN and Gabra2. A small number of cells seemed, however, to express long processes staining positive for both NeuN and Gabra2.

An expression study in rat brain has shown strong expression of PGC-1α in GABAergic neurons in Hc and Cx. (Lucas et al. 2010) It has been suggested that PGC-1α is an essential influencer of survival and homeostasis maintenance in GABAergic neurons in developing and adult rat brains. (Cowell, Blake & Russell 2007, Lucas et al. 2010)

We hypothesized that this relationship may be important in PGC-1α tg mice and have a possible involvement in conferring neuroprotective properties of PGC-1α overexpression.

In immunostainings of hippocampal sections of wt mice, virtually all Gabra2 positive neurons were found to be expressing PGC-1α. The signals appeared to be closely colocalized, and a large fraction of the signals were directly overlapping, as shown in figure 26 B. This pattern was observed as well in hippocampi of tg mice. However, and unexpectedly, in PGC-1α tg mice, Gabra2 positive signals appeared outside the soma in the shape of prolonged processes and were observed mainly in Hc (compare figure 26 C). All extrasomatic Gabra2 signals overlapped with PGC-1α positive staining. Stainings suggest a higher number of hippocampal neurons expressing Gabra2 in the tg as compared to the wt mice. However, this needs to be studied in quantitative manner in the future.

Similarly, we studied the expression of $GABA_A$ receptor subunits in cortical samples of tg mice. Expression of Gabra2 is highly increased in Cx, averaging 1.72 ± 0.41. The high standard deviation originates from individual differences in expression levels among the tg mice. In contrast, Gabrg2 is underexpressed (0.74 ± 0.09). This parallels the findings in Hc, even though the increase in Gabra2 is not as pronounced in Cx of tg mice.

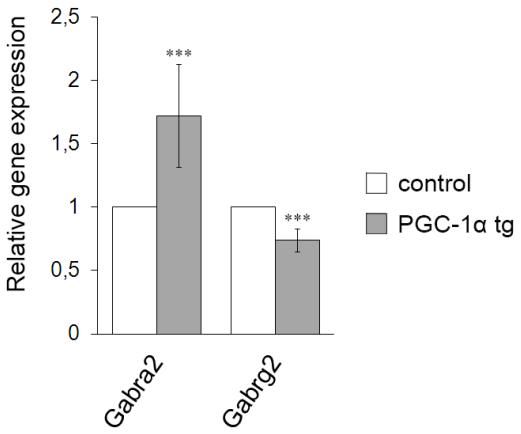

Figure 27 Gene expression analysis for Gabra2 and Gabrg2 in Cx. Relative expression levels in Cx of PGC-1α tg mice, ± stdev. Stars denote statistical significance compared to wt controls (*** p<0.001).

Similar analyses of expression patterns on the protein level were performed in cortical sections. The expression of Gabra2 in the Cx of PGC-1α tg mice appeared very similar to the hippocampal staining pattern: in both controls and tg animals, Gabra2 was colocalized with the neuronal marker NeuN, being expressed in the nuclei of neurons (compare figure 28 A).

Gabra2 positive neurons were closely colocalized with PGC-1α. Virtually all of the nuclei of GABAergic neurons showed strong PGC-1α expression. Representative images are shown in figure 28 B.

In addition, some of the neurons appeared to be expressing long processes with strong Gabra2 staining and positive signal for PGC-1α.

Interestingly, the number of Gabra2 positive neurons in Cx seemed to be considerably higher in tg than in wt mice. This remains to be assessed in more detail in future experiments.

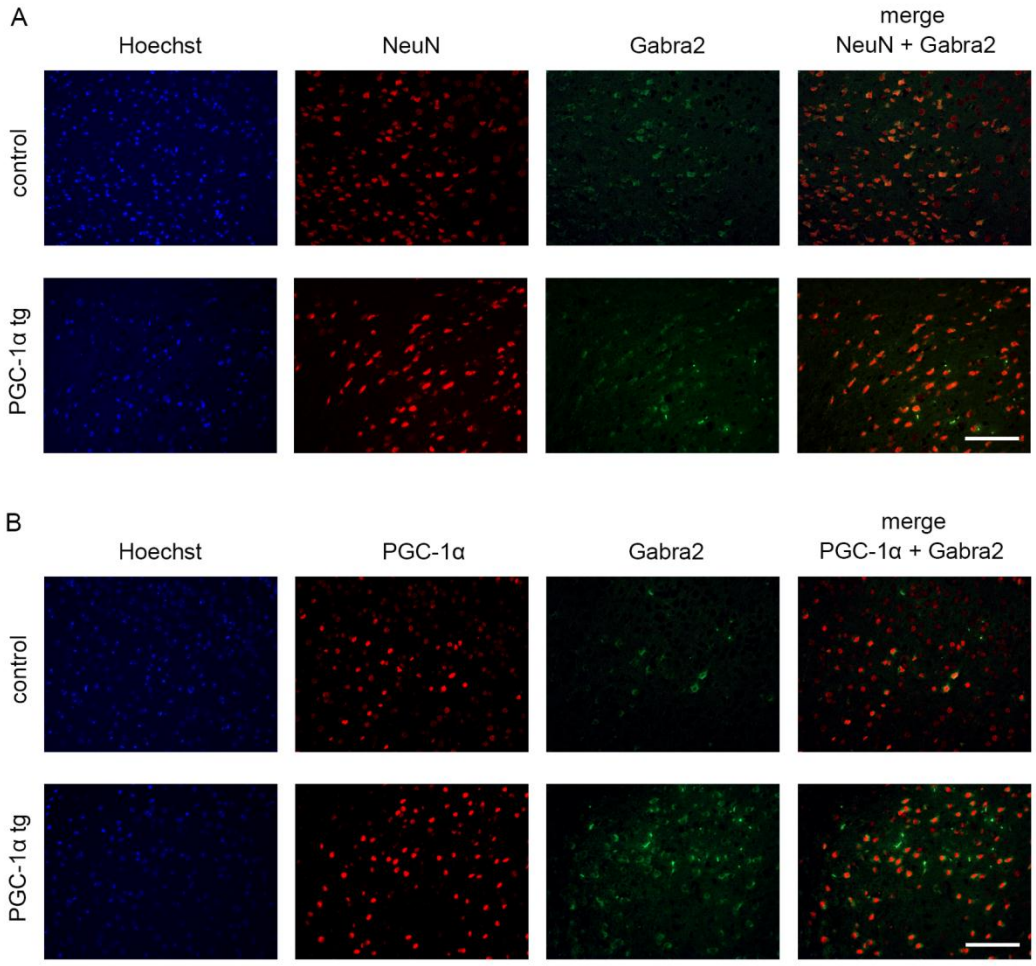

Figure 28 Localization analysis for Gabra2 in Cx. A. Colocalization analysis for NeuN and Gabra2. Immunostainings for the neuronal marker NeuN and Gabra2. **B. Colocalization analysis for PGC-1α and Gabra2.** Immunostainings for PGC-1α and Gabra2. Upper panels (control): wt controls, lower panels (PGC-1α tg): PGC-1α tg mice. 20x magnification, scale bar 100μm.

5. Discussion

5.1. Technical aspects of the system

5.1.1. Comparison of microarray and qPCR

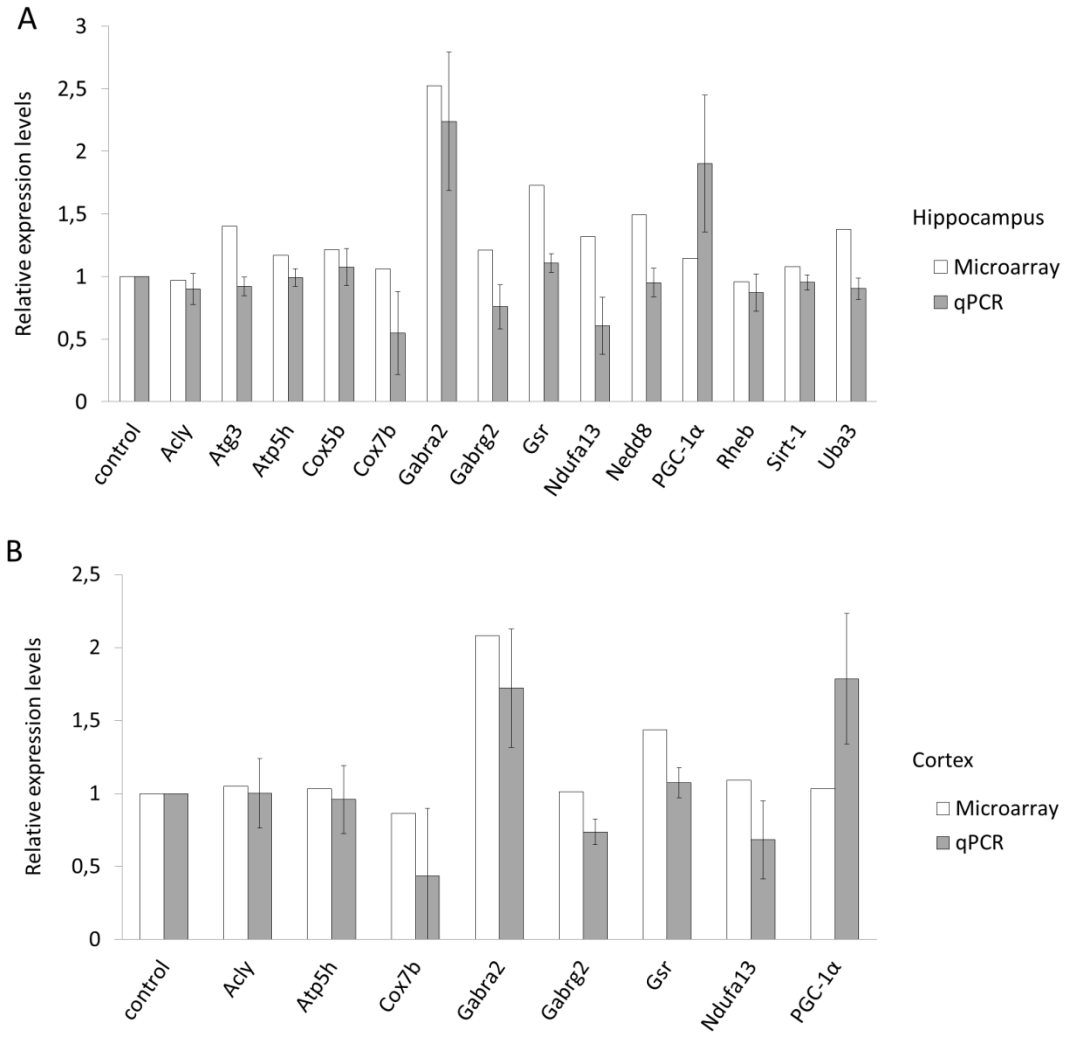

Figure 29 Comparison of relative gene expression levels measured by microarray and qPCR A. in Hc, B. in Cx.

Comparing the initial screening results found in the microarray based study with the expression levels measured by qPCR, it is obvious that the results differ partly. For the genes with the most pronounced differential regulation, the tendencies could be confirmed by qPCR, even though the expression values differ somewhat.

In direct comparison, the expression levels measured by microarray appear to be somewhat higher than the values measured with qPCR throughout most of the genes, as shown figure 29. Strikingly, the expression of PGC-1α was underestimated by the microarray. For genes with very small increase or reduction in expression levels, the

findings of microarray and qPCR are somewhat contradictory. Since the microarray appears to generally estimate the expression values higher than the qPCR based system, small increases identified with the microarray screening consistently translate to slightly decreased mRNA levels in the qPCR measurements.

The differences in gene expression levels seem to be due to a systematic difference. As described in chapter 4.1., the qPCR system setup used for gene expression measurements in this study was optimized for each of the target genes. This ensures highly reliable, specific targeting of the genes of interest and rules out false positives due to unspecific binding. The qPCR setup was optimized to be highly specific for mRNAs transcribed from the genes of interest. Primers were designed to target mRNAs in a highly specific manner, and gene expression levels were normalized to average values of two reference genes known to be expressed at similar, stable levels in the control and tg mice. The normalization levels out small differences in cDNA input amounts and pipetting errors. Crossreactivity with other mRNAs, which would result in unspecific binding and false positive results, was ruled out. Due to the sequence recognition setup in microarrays, crossreactivity between different targets is more likely. (Draghici et al. 2006)

Microarrays are still mainly used for screening purposes, as was the case in this study. The main advantage of microarrays is a large-scale, rapid screening process, whereas qPCR is more labor-intensive, but produces more reliable results. (VanGuilder, Vrana & Freeman 2008, Draghici et al. 2006)

A biological aspect to be considered is that the detection of differential regulation is more difficult in mature neurons than in many other cells. This is based on the fact that mature neurons generally undergo very small changes in expression activity (Elstner et al. 2011) Due to the small effect size, it is difficult to reliably detect changes.

For these reasons, the qPCR based system may be considered more reliable in detecting small differences in expression levels, and more suitable for expression analysis in brain samples.

5.1.2. Biological factors to be taken into account

5.1.2.1. Interpretation of mRNA expression data

This study aimed at further characterizing gene expression networks in Hc and Cx of PGC-1α tg mice. The characterization was focused on the mRNA expression.

However, differential expression is not necessarily translated into equal changes in protein levels. The expression values found in this study provide a measure to identify PGC-1α target genes. Equally, it is possible to draw conclusions about the effect of PGC-1α overexpression on the studied gene expression networks and their transcriptional activity.

Adding to previous findings, our results suggest that the changes in mRNA levels reported here are also reflected by differential expression on the protein level. (Mudo et al. 2012)

In this study, we aimed at identifying targets of PGC-1α regulation that are differentially expressed on the mRNA level. Conclusions about the influence of the expression changes reported here on the activity and functionality of the molecular pathways, however, are preliminary and will have to be assessed experimentally.

5.1.2.2. Mitochondrial biology

In this study, expression levels were normalized to the average expression of two reference genes located in the cytosol of cells. The expression levels can therefore be considered as an average per cell.

PGC-1α has been shown to regulate mitochondrial density in neurons. (Wareski et al. 2009) At present, it is only possible to speculate about the influences of PGC-1α on mitochondrial number in neurons of the PGC-1α tg mouse line. It is well possible that PGC-1α overexpressing neurons possess higher numbers of mitochondria. It is conceivable that PGC-1α not only influences the mitochondrial number, but possibly exerts its neuroprotective effects via enhancing mitochondrial functional state.

For future projects, it would be interesting to measure protein levels, normalized to the number of mitochondria per cell, in order to estimate the functional state of mitochondria.

5.1.2.3. Cell population for measurements

Whole tissue hippocampal and cortical samples were used for analysis. As a consequence, the reported values reflect an average of expression patterns over neurons as well as glial cells. Expression of exogenous PGC-1α is restricted to neurons via the use of the specific Thy1.2 promoter in the tg mice. (Vidal et al. 1990, Caroni 1997) Therefore, the changes in gene expression levels reported in this study can be attributed to PGC-1α regulated changes in neuronal gene expression networks. However, glial cells may as well be influenced by expression patterns in adjacent neurons, which may result in changes in gene expression. This possible confounding factor can be excluded by studying gene expression specifically in neurons of PGC-1α tg mice.

DA neurons are more vulnerable to dysregulations in cellular homeostasis than other neurons. They are the predominant target of pathological changes in both models as well as clinical studies of neurodegeneration in PD. (Zheng et al. 2010)

This points towards a particularly important role of PGC-1α regulated gene expression networks in DA neurons. For further analysis of the role of PGC-1α expression in the cell viability of DA neurons, specific analysis of mRNA and protein levels could be performed.

5.2. Implications for PGC-1α regulated molecular pathways

5.2.1. Expression analysis of PGC-1α

This study has confirmed the overexpression of PGC-1α in Hc and Cx of tg mice on the mRNA level. As shown immunohistochemically, transgene driven expression of PGC-1α results in translation into protein, and the presence of exogenous PGC-1α in hippocampal and cortical neurons of PGC-1α tg mice was confirmed.

This reflects the findings reported by Mudò and coworkers. In their study characterizing the PGC-1α tg mouse line, increased protein levels of PGC-1α were found in striatum and substantia nigra. (Mudo et al. 2012)

The subcellular localization patterns of tg PGC-1α remain to studied further, since immunostainings showed a predominant localization in close proximity of, rather than within, the nucleus.

Another aspect to be studied are the levels of active PGC-1α. Protein expression driven by the transgene was confirmed qualitatively in this study. However, the mRNA expression levels do not necessarily reflect the protein levels. Translation of mRNA into protein may be regulated in a way as to change the relative contribution of the transgene expression. Another interesting aspect for further characterization are the relative amounts of endogenous and transgene-driven mRNA and their contributions to translation into protein.

Future studies will be aimed at quantifying PGC-1α protein levels. Furthermore, the activity levels of PGC-1α in the tg mice remains to be studied. As reviewed in chapter 1.3.1., PGC-1α activity is regulated not only on the transcriptional level, but on a shorter term by a host of posttranslational modifications. The most prominent modification mechanism is activation by deacetylation via Sirt-1. (Canto, Auwerx 2009) For these reasons, PGC-1α protein levels would not necessarily reflect the activity of PGC-1α in a cell, and the influence and balance between activating and inactivating posttranslational modifications has to be taken into account.

5.2.2. Partial downregulation of mitochondrial metabolic enzymes

The expression levels of mitochondrial respiratory chain complex subunits were either unchanged or decreased. A pronounced downregulation was found in PGC-1α tg mouse Hc and Cx for complex I (NADH dehydrogenase 1α) subunit 13d, and complex IV (cytochrome c oxidase) subunit 7b. Additionally, citrate lyase was slightly underexpressed in hippocampal samples. The remaining genes related to ATP production were unchanged in tg mice.

Mitochondria in brains of PGC-1α tg mice possess an enhanced metabolic capacity. (Mudo et al. 2012) Together with the downregulation of electron transport chain enzyme subunits, this may be suggesting a more efficient respiration in tg mice.

It is, at least in hindsight, not surprising that mitochondrial respiratory chain complexes are downregulated in PGC-1α tg mice. The most pronounced decrease in mRNA levels was observed for subunits of mitochondrial electron transport chain complexes IV and I, known to be among the main contributors to oxidative stress. (Balaban, Nemoto & Finkel 2005, Nicholls 2002) It is likely that the respiratory chain activity undergoes adaptative changes. Merely increasing oxidative

phosphorylation activity via PGC-1α would be paralleled by an increase in ROS production and ultimately cause harm to the cells. We hypothesize that the increased respiratory rate control observed in mitochondria of PGC-1α tg mice is based on an enhanced functional state of the electron transport chain rather than an increase in the expression of enzymes. Via this mechanism, mitochondria can possibly improve efficiency of ATP production, but at the same time maintain low amounts of ROS production. (Puigserver et al. 1998)

In contrast, acute overexpression of PGC-1α in cultured cells has been reported to entail increased expression of mitochondrial energy metabolism pathways. (Puigserver et al. 1998, Wu et al. 1999) Forced overexpression of PGC-1α at high levels may, however, not be directly comparable to the changes in PGC-1α tg mice. PGC-1α levels in brain neurons of PGC-1α tg mice are enhanced, but still within a physiological range. (Lindholm et al. 2012)

The long-term exposure to increased PGC-1α levels may induce feedback loops in neurons. This is probably the case in the PGC-1α tg mice, especially in view with the tight regulation of mitochondrial homeostasis mediated by PGC-1α.

Compensatory mechanisms have been reported to be an effective response to PGC-1α depletion in mice. (St-Pierre et al. 2006) We hypothesize that sustained PGC-1α overexpression equally entails changes in pathways under influence of PGC-1α. The slight downregulation of Sirt-1 as immediate activity regulator of PGC-1α activity may be a hint in the same direction.

For future studies, this is going to be assessed by measuring age-dependent gene expression changes in PGC-1α tg mice.

5.2.3. Upregulation of the mitochondrial antioxidant system

The mitochondrial antioxidant glutathione reductase was upregulated in Hc and Cx of PGC-1α tg mice. This parallels enhanced expression of several other mitochondrial antioxidants shown by Mudo et al in SNc of tg mice. (Mudo et al. 2012) This upregulation suggests an increased production of antioxidants and is in line with increased antioxidant expression as a response to oxidative stress, which is blunted upon PGC-1α depletion in murine brain neurons. (St-Pierre et al. 2006) The increased expression of antioxidants is likely contributing to an enhanced ability of

PGC-1α overexpressing neurons to scavenge ROS, contributing to an improved functional state of neurons.

5.2.4. Expression analysis of nonmitochondrial pathways implied in Parkinson's Disease

In Hc of PGC-1α mice, decreased expression levels of some non-mitochondrial proteins involved in handling of dysfunctional proteins were found.

mTOR signaling and autophagy associated proteins Rheb and Atg3 were slightly, but significantly underexpressed in Hc of PGC-1α tg mice. Cell cycle progression mediator Nedd8 did not appear to be influenced on the mRNA expression levels by PGC-1α overexpression. The regulator of Nedd8 activity, Uba3, was slightly downregulated.

This unexpected downregulation may be due to feedback loops induced upon sustained PGC-1α overexpression. The translation into proteins and their activity remains to be studied in order to place these findings in a physiological context.

5.2.5. Differential expression of $GABA_A$ receptor subunits

In this study, gene expression determining the subunit composition of $GABA_A$ receptor, the predominant mediator for fast inhibitory signaling, was found to be altered in PGC-1α tg mice. The subunit composition, particularly of the α subunits, influences the subcellular localization of $GABA_A$ receptors. This, in turn, allows conclusions about the signaling properties. α2 subunit containing receptors are contributing to synaptic inhibition. (Hines et al. 2012, Wu et al. 2012) The strong shift towards subunit α2 expression may hint at a higher number of α2 containing $GABA_A$ receptors, located at synapses. Our findings suggest an enhanced production of receptors mediating fast, synaptic inhibition in the PGC-1α tg mice.

GABAergic signaling pathways are impaired with aging and changes in $GABA_A$ receptor subunit composition have been reported in connection with several neuropathologies and neurodegenerative diseases. (Elstner et al. 2011, Luchetti, Huitinga & Swaab 2011)

Moreover, PGC-1α is strongly expressed in GABAergic interneurons throughout the rat brain during development. It has been suggested that PGC-1α expression during development mediates mitochondrial biogenesis and activity, which is important for formation of synaptic contacts. Furthermore, it has been proposed that PGC-1α acts on GABAergic neurons by influencing glucose metabolism. (Cowell, Blake & Russell 2007) In line with this, our findings suggest a link between neuroprotection and the expression of $GABA_A$ receptor subunits. Our findings imply that an increased number of neurons are targeted by GABAergic synaptic inhibitory signaling. The IHC staining results indicate an increase in the number of Gabra2 expressing neurons. A conceivable explanation is that PGC-1α possibly enhances the functional state of GABAergic neurons and their interactions via synaptic signals by promoting the expression of $GABA_A$ receptors. These findings may imply protection against glutamate mediated excitotoxicity via increased inhibitory signaling. Possibly, this is related to the role of PGC-1α regulating vulnerability of neurons towards excitotoxicity. (Cowell, Blake & Russell 2007, Hines et al. 2012, Lucas et al. 2010, Soriano et al. 2011)

5.3. Conclusions and future prospects

The aim of this Master's thesis study was to measure gene expression on the mRNA levels for a set of genes and identify gene networks with differentially regulated expression patterns in PGC-1α tg mice as compared to wt controls.

PGC-1α overexpression in tg mice was confirmed on the mRNA level, and translation to protein was confirmed.

Our results show that PGC-1α overexpression in brain neurons is associated with significant changes in gene expression patterns. This concerns mitochondrial oxidative metabolism and antioxidant systems. Further, non-mitochondrial pathways showing alterations in gene expression in association with PGC-1α overexpression were GABAergic receptor signaling, autophagy, and contributors to cell cycle regulation.

In keeping with previous studies of the physiology of brain neurons of PGC-1α tg mice, our finding suggest that PGC-1α overexpression may cause gene expression changes that enhance the functional state of hippocampal and cortical neurons.

Our results suggest that PGC-1α may be able to alter gene expression networks in a way to enhance mitochondrial functional state and confer protection against oxidative stress and energetic failure.

In accordance with previous reports, the studies presented in this Master's thesis contribute to forming a coherent picture of the neuroprotective influences mediated by PGC-1α controlled gene expression networks. PGC-1α and related coactivators on the one hand are able to mediate responses to increased energetic demands and to maintain a level of energy supply by regulating oxidative phosphorylation. On the other hand, PGC-1α also is involved in scavenging the increased amounts of oxidants that are being generated as a byproduct of enhanced metabolic activity, ensuring a stable energetic and oxidative cellular homeostasis. (Wu et al. 1999, Rohas et al. 2007)

Future directions for this project will predominantly be aimed at a more thorough characterization of the PGC-1α tg mouse line in the focus of this Master's Thesis study. As a first step, PGC-1α protein expression and activity levels have to be studied. For future studies, it will be important to determine whether gene expression patterns are paralleled by translation protein, how the dynamics of the processes and mitochondrial physiology are affected.

The findings reported here reflect the complex interactions in which PGC-1α is involved. This equally concerns regulation of PGC-1α expression and activity, as interactions between the PGC-1α regulated processes. The complexity of the PGC-1α regulated interactions that maintain cellular homeostasis shows how tightly regulated and thoroughly maintained these pathways are.

In view with a role of PGC-1α in neuroprotection, it is clear that neurodegeneration, and particularly PD, is the result of a host of disturbances in multiple cellular functions and their mutual interactions. For this reason, it is certainly difficult to stop pathogenesis by intervening at one single point. For neuroprotective treatments, it is more feasible to halt disease progression by targeting multiple pathways simultaneously.

PGC-1α may be a suitable axis of regulation, being is the pivotal point translating a number of environmental signals into changes in several pathways that ultimately all contribute to maintain intracellular homeostasis. Furthermore, PGC-1α can relatively

easily be modulated by small molecular compounds, such as the polyphenol resveratrol (RSV). (Lagouge et al. 2006)

Screening for mild dysregulations in PD affected pathways early in disease progression might be used as an indicator for starting neuroprotective treatment. (Zheng et al. 2010) Subsequently, boosting PGC-1α activity may influence a number of pathways and positively affect the functional state of brain neurons to stabilize the functional state of predominantly, but not only, the nigrostriatal system. Additional brain areas have been implicated in PD, such as the Hc, thought to be having a role in neuroregeneration. (Marxreiter, Regensburger & Winkler 2013)

By pharmacologically targeting PGC-1α and enhancing the neuroprotective effects via PGC-1α controlled pathways, neurons could be protected from degeneration, and possibly the disease progression could be slowed. On the long term, this can contribute to establishing a curative treatment for PD.

References

Abou-Sleiman, P.M., Muqit, M.M. & Wood, N.W. 2006, "Expanding insights of mitochondrial dysfunction in Parkinson's disease", *Nature reviews.Neuroscience,* vol. 7, no. 3, pp. 207-219.

Andrews, Z.B., Diano, S. & Horvath, T.L. 2005, "Mitochondrial uncoupling proteins in the CNS: in support of function and survival", *Nature reviews.Neuroscience,* vol. 6, no. 11, pp. 829-840.

Arduino, D.M., Esteves, A.R., Oliveira, C.R. & Cardoso, S.M. 2010, "Mitochondrial metabolism modulation: a new therapeutic approach for Parkinson's disease", *CNS & neurological disorders drug targets,* vol. 9, no. 1, pp. 105-119.

Atlante, A., Calissano, P., Bobba, A., Giannattasio, S., Marra, E. & Passarella, S. 2001, "Glutamate neurotoxicity, oxidative stress and mitochondria", *FEBS letters,* vol. 497, no. 1, pp. 1-5.

Balaban, R.S., Nemoto, S. & Finkel, T. 2005, "Mitochondria, oxidants, and aging", *Cell,* vol. 120, no. 4, pp. 483-495.

Beal, M.F. 2005, "Mitochondria take center stage in aging and neurodegeneration", *Annals of Neurology,* vol. 58, no. 4, pp. 495-505.

Beal, M.F. 2003, "Mitochondria, oxidative damage, and inflammation in Parkinson's disease", *Annals of the New York Academy of Sciences,* vol. 991, pp. 120-131.

Beal, M.F. 1998, "Excitotoxicity and nitric oxide in Parkinson's disease pathogenesis", *Annals of Neurology,* vol. 44, no. 3 Suppl 1, pp. S110-4.

Betarbet, R., Sherer, T.B., MacKenzie, G., Garcia-Osuna, M., Panov, A.V. & Greenamyre, J.T. 2000, "Chronic systemic pesticide exposure reproduces features of Parkinson's disease", *Nature neuroscience,* vol. 3, no. 12, pp. 1301-1306.

Blandini, F. 2010, "An update on the potential role of excitotoxicity in the pathogenesis of Parkinson's disease", *Functional neurology,* vol. 25, no. 2, pp. 65-71.

Brotchie, J. & Fitzer-Attas, C. 2009, "Mechanisms compensating for dopamine loss in early Parkinson disease", *Neurology,* vol. 72, no. 7 Suppl, pp. S32-8.

Canto, C. & Auwerx, J. 2009, "PGC-1alpha, SIRT1 and AMPK, an energy sensing network that controls energy expenditure", *Current opinion in lipidology,* vol. 20, no. 2, pp. 98-105.

Caroni, P. 1997, "Overexpression of growth-associated proteins in the neurons of adult transgenic mice", *Journal of neuroscience methods,* vol. 71, no. 1, pp. 3-9.

Chypre, M., Zaidi, N. & Smans, K. 2012, "ATP-citrate lyase: a mini-review", *Biochemical and biophysical research communications,* vol. 422, no. 1, pp. 1-4.

Clark, J. & Simon, D.K. 2009, "Transcribe to survive: transcriptional control of antioxidant defense programs for neuroprotection in Parkinson's disease", *Antioxidants & redox signaling,* vol. 11, no. 3, pp. 509-528.

Cohen, G. 2000, "Oxidative stress, mitochondrial respiration, and Parkinson's disease", *Annals of the New York Academy of Sciences,* vol. 899, pp. 112-120.

Cohen, G., Farooqui, R. & Kesler, N. 1997, "Parkinson disease: a new link between monoamine oxidase and mitochondrial electron flow", *Proceedings of the National Academy of Sciences of the United States of America,* vol. 94, no. 10, pp. 4890-4894.

Cohen, G. & Kesler, N. 1999a, "Monoamine oxidase and mitochondrial respiration", *Journal of neurochemistry,* vol. 73, no. 6, pp. 2310-2315.

Cohen, G. & Kesler, N. 1999b, "Monoamine oxidase inhibits mitochondrial respiration", *Annals of the New York Academy of Sciences,* vol. 893, pp. 273-278.

Cowell, R.M., Blake, K.R. & Russell, J.W. 2007, "Localization of the transcriptional coactivator PGC-1alpha to GABAergic neurons during maturation of the rat brain", *The Journal of comparative neurology*, vol. 502, no. 1, pp. 1-18.

Dauer, W. & Przedborski, S. 2003, "Parkinson's disease: mechanisms and models", *Neuron*, vol. 39, no. 6, pp. 889-909.

Dexter, D.T. & Jenner, P. 2013, "Parkinson disease: from pathology to molecular disease mechanisms", *Free radical biology & medicine*, .

Dorak, M.T. 2006, *Real-time PCR*, Taylor & Francis, New York, NY.

Draghici, S., Khatri, P., Eklund, A.C. & Szallasi, Z. 2006, "Reliability and reproducibility issues in DNA microarray measurements", *Trends in genetics : TIG*, vol. 22, no. 2, pp. 101-109.

Duchen, M.R. 2004, "Mitochondria in health and disease: perspectives on a new mitochondrial biology", *Molecular aspects of medicine*, vol. 25, no. 4, pp. 365-451.

Elstner, M., Morris, C.M., Heim, K., Bender, A., Mehta, D., Jaros, E., Klopstock, T., Meitinger, T., Turnbull, D.M. & Prokisch, H. 2011, "Expression analysis of dopaminergic neurons in Parkinson's disease and aging links transcriptional dysregulation of energy metabolism to cell death", *Acta Neuropathologica*, vol. 122, no. 1, pp. 75-86.

Esterbauer, H., Oberkofler, H., Krempler, F. & Patsch, W. 1999, "Human peroxisome proliferator activated receptor gamma coactivator 1 (PPARGC1) gene: cDNA sequence, genomic organization, chromosomal localization, and tissue expression", *Genomics*, vol. 62, no. 1, pp. 98-102.

Fernandez-Marcos, P.J. & Auwerx, J. 2011, "Regulation of PGC-1alpha, a nodal regulator of mitochondrial biogenesis", *The American Journal of Clinical Nutrition*, vol. 93, no. 4, pp. 884S-90.

Gong, L. & Yeh, E.T. 1999, "Identification of the activating and conjugating enzymes of the NEDD8 conjugation pathway", *The Journal of biological chemistry*, vol. 274, no. 17, pp. 12036-12042.

Hines, R.M., Davies, P.A., Moss, S.J. & Maguire, J. 2012, "Functional regulation of GABAA receptors in nervous system pathologies", *Current opinion in neurobiology*, vol. 22, no. 3, pp. 552-558.

Holopainen, I.E. & Lauren, H.B. 2003, "Neuronal activity regulates GABAA receptor subunit expression in organotypic hippocampal slice cultures", *Neuroscience*, vol. 118, no. 4, pp. 967-974.

Imai, S., Johnson, F.B., Marciniak, R.A., McVey, M., Park, P.U. & Guarente, L. 2000, "Sir2: an NAD-dependent histone deacetylase that connects chromatin silencing, metabolism, and aging", *Cold Spring Harbor symposia on quantitative biology*, vol. 65, pp. 297-302.

Jankovic, J. 2008, "Parkinson's disease: clinical features and diagnosis", *Journal of neurology, neurosurgery, and psychiatry*, vol. 79, no. 4, pp. 368-376.

Jeninga, E.H., Schoonjans, K. & Auwerx, J. 2010, "Reversible acetylation of PGC-1: connecting energy sensors and effectors to guarantee metabolic flexibility", *Oncogene*, vol. 29, no. 33, pp. 4617-4624.

Jenner, P. 2004, "Preclinical evidence for neuroprotection with monoamine oxidase-B inhibitors in Parkinson's disease", *Neurology*, vol. 63, no. 7 Suppl 2, pp. S13-22.

Jenner, P. 2003, "Oxidative stress in Parkinson's disease", *Annals of Neurology*, vol. 53 Suppl 3, pp. S26-36; discussion S36-8.

Jenner, P. & Olanow, C.W. 2006, "The pathogenesis of cell death in Parkinson's disease", *Neurology*, vol. 66, no. 10 Suppl 4, pp. S24-36.

Kamitani, T., Kito, K., Nguyen, H.P. & Yeh, E.T. 1997, "Characterization of NEDD8, a developmentally down-regulated ubiquitin-like protein", *The Journal of biological chemistry*, vol. 272, no. 45, pp. 28557-28562.

Kelly, D.P. & Scarpulla, R.C. 2004, "Transcriptional regulatory circuits controlling mitochondrial biogenesis and function", *Genes & development*, vol. 18, no. 4, pp. 357-368.

Kim, I., Rodriguez-Enriquez, S. & Lemasters, J.J. 2007, "Selective degradation of mitochondria by mitophagy", *Archives of Biochemistry and Biophysics*, vol. 462, no. 2, pp. 245-253.

Kowaltowski, A.J., de Souza-Pinto, N.C., Castilho, R.F. & Vercesi, A.E. 2009, "Mitochondria and reactive oxygen species", *Free radical biology & medicine*, vol. 47, no. 4, pp. 333-343.

Kukidome, D., Nishikawa, T., Sonoda, K., Imoto, K., Fujisawa, K., Yano, M., Motoshima, H., Taguchi, T., Matsumura, T. & Araki, E. 2006, "Activation of AMP-activated protein kinase reduces hyperglycemia-induced mitochondrial reactive oxygen species production and promotes mitochondrial biogenesis in human umbilical vein endothelial cells", *Diabetes*, vol. 55, no. 1, pp. 120-127.

Lagouge, M., Argmann, C., Gerhart-Hines, Z., Meziane, H., Lerin, C., Daussin, F., Messadeq, N., Milne, J., Lambert, P., Elliott, P., Geny, B., Laakso, M., Puigserver, P. & Auwerx, J. 2006, "Resveratrol improves mitochondrial function and protects against metabolic disease by activating SIRT1 and PGC-1alpha", *Cell*, vol. 127, no. 6, pp. 1109-1122.

Lee, J., Giordano, S. & Zhang, J. 2012, "Autophagy, mitochondria and oxidative stress: cross-talk and redox signalling", *The Biochemical journal*, vol. 441, no. 2, pp. 523-540.

Leone, T.C., Lehman, J.J., Finck, B.N., Schaeffer, P.J., Wende, A.R., Boudina, S., Courtois, M., Wozniak, D.F., Sambandam, N., Bernal-Mizrachi, C., Chen, Z., Holloszy, J.O., Medeiros, D.M., Schmidt, R.E., Saffitz, J.E., Abel, E.D., Semenkovich, C.F. & Kelly, D.P. 2005, "PGC-1alpha deficiency causes multi-system energy metabolic derangements: muscle dysfunction, abnormal weight control and hepatic steatosis", *PLoS biology*, vol. 3, no. 4, pp. e101.

Lin, J., Handschin, C. & Spiegelman, B.M. 2005, "Metabolic control through the PGC-1 family of transcription coactivators", *Cell metabolism*, vol. 1, no. 6, pp. 361-370.

Lin, J., Wu, P.H., Tarr, P.T., Lindenberg, K.S., St-Pierre, J., Zhang, C.Y., Mootha, V.K., Jager, S., Vianna, C.R., Reznick, R.M., Cui, L., Manieri, M., Donovan, M.X., Wu, Z., Cooper, M.P., Fan, M.C., Rohas, L.M., Zavacki, A.M., Cinti, S., Shulman, G.I., Lowell, B.B., Krainc, D. & Spiegelman, B.M. 2004, "Defects in adaptive energy metabolism with CNS-linked hyperactivity in PGC-1alpha null mice", *Cell*, vol. 119, no. 1, pp. 121-135.

Lin, M.T. & Beal, M.F. 2006, "Mitochondrial dysfunction and oxidative stress in neurodegenerative diseases", *Nature*, vol. 443, no. 7113, pp. 787-795.

Lindholm, D., Eriksson, O., Makela, J., Belluardo, N. & Korhonen, L. 2012, "PGC-1alpha: a master gene that is hard to master", *Cellular and molecular life sciences : CMLS*, vol. 69, no. 15, pp. 2465-2468.

Livak, K.J. & Schmittgen, T.D. 2001, "Analysis of relative gene expression data using real-time quantitative PCR and the 2(-Delta Delta C(T)) Method", *Methods (San Diego, Calif.)*, vol. 25, no. 4, pp. 402-408.

Lotharius, J. & Brundin, P. 2002, "Pathogenesis of Parkinson's disease: dopamine, vesicles and alpha-synuclein", *Nature reviews.Neuroscience*, vol. 3, no. 12, pp. 932-942.

Lucas, E.K., Markwardt, S.J., Gupta, S., Meador-Woodruff, J.H., Lin, J.D., Overstreet-Wadiche, L. & Cowell, R.M. 2010, "Parvalbumin deficiency and GABAergic dysfunction in mice lacking PGC-1alpha", *The Journal of neuroscience : the official journal of the Society for Neuroscience*, vol. 30, no. 21, pp. 7227-7235.

Luchetti, S., Huitinga, I. & Swaab, D.F. 2011, "Neurosteroid and GABA-A receptor alterations in Alzheimer's disease, Parkinson's disease and multiple sclerosis", *Neuroscience*, vol. 191, pp. 6-21.

Ma, D., Li, S., Lucas, E.K., Cowell, R.M. & Lin, J.D. 2010, "Neuronal inactivation of peroxisome proliferator-activated receptor gamma coactivator 1alpha (PGC-1alpha) protects mice from diet-induced obesity and leads to degenerative lesions", *The Journal of biological chemistry,* vol. 285, no. 50, pp. 39087-39095.

Marxreiter, F., Regensburger, M. & Winkler, J. 2013, "Adult neurogenesis in Parkinson's disease", *Cellular and molecular life sciences : CMLS,* vol. 70, no. 3, pp. 459-473.

Meredith, G.E., Totterdell, S., Beales, M. & Meshul, C.K. 2009, "Impaired glutamate homeostasis and programmed cell death in a chronic MPTP mouse model of Parkinson's disease", *Experimental neurology,* vol. 219, no. 1, pp. 334-340.

Meredith, G.E., Totterdell, S., Potashkin, J.A. & Surmeier, D.J. 2008, "Modeling PD pathogenesis in mice: advantages of a chronic MPTP protocol", *Parkinsonism & related disorders,* vol. 14 Suppl 2, pp. S112-5.

Moore, D.J., West, A.B., Dawson, V.L. & Dawson, T.M. 2005, "Molecular pathophysiology of Parkinson's disease", *Annual Review of Neuroscience,* vol. 28, pp. 57-87.

Mootha, V.K., Handschin, C., Arlow, D., Xie, X., St Pierre, J., Sihag, S., Yang, W., Altshuler, D., Puigserver, P., Patterson, N., Willy, P.J., Schulman, I.G., Heyman, R.A., Lander, E.S. & Spiegelman, B.M. 2004, "Erralpha and Gabpa/b specify PGC-1alpha-dependent oxidative phosphorylation gene expression that is altered in diabetic muscle", *Proceedings of the National Academy of Sciences of the United States of America,* vol. 101, no. 17, pp. 6570-6575.

Mudo, G., Makela, J., Di Liberto, V., Tselykh, T.V., Olivieri, M., Piepponen, P., Eriksson, O., Malkia, A., Bonomo, A., Kairisalo, M., Aguirre, J.A., Korhonen, L., Belluardo, N. & Lindholm, D. 2012, "Transgenic expression and activation of PGC-1alpha protect dopaminergic neurons in the MPTP mouse model of Parkinson's disease", *Cellular and molecular life sciences : CMLS,* vol. 69, no. 7, pp. 1153-1165.

Murphy, A.N., Fiskum, G. & Beal, M.F. 1999, "Mitochondria in neurodegeneration: bioenergetic function in cell life and death", *Journal of cerebral blood flow and metabolism : official journal of the International Society of Cerebral Blood Flow and Metabolism,* vol. 19, no. 3, pp. 231-245.

Nicholls, D.G. 2002, "Mitochondrial function and dysfunction in the cell: its relevance to aging and aging-related disease", *The international journal of biochemistry & cell biology,* vol. 34, no. 11, pp. 1372-1381.

Nicholls, D.G., Johnson-Cadwell, L., Vesce, S., Jekabsons, M. & Yadava, N. 2007, "Bioenergetics of mitochondria in cultured neurons and their role in glutamate excitotoxicity", *Journal of neuroscience research,* vol. 85, no. 15, pp. 3206-3212.

Nunnari, J. & Suomalainen, A. 2012, "Mitochondria: in sickness and in health", *Cell,* vol. 148, no. 6, pp. 1145-1159.

Pfaffl, M.W. 2001, "A new mathematical model for relative quantification in real-time RT-PCR", *Nucleic acids research,* vol. 29, no. 9, pp. e45.

Poewe, W. 2008, "Non-motor symptoms in Parkinson's disease", *European journal of neurology : the official journal of the European Federation of Neurological Societies,* vol. 15 Suppl 1, pp. 14-20.

Przedborski, S., Tieu, K., Perier, C. & Vila, M. 2004, "MPTP as a mitochondrial neurotoxic model of Parkinson's disease", *Journal of Bioenergetics and Biomembranes,* vol. 36, no. 4, pp. 375-379.

Puigserver, P. & Spiegelman, B.M. 2003, "Peroxisome proliferator-activated receptor-gamma coactivator 1 alpha (PGC-1 alpha): transcriptional coactivator and metabolic regulator", *Endocrine reviews,* vol. 24, no. 1, pp. 78-90.

Puigserver, P., Wu, Z., Park, C.W., Graves, R., Wright, M. & Spiegelman, B.M. 1998, "A cold-inducible coactivator of nuclear receptors linked to adaptive thermogenesis", *Cell,* vol. 92, no. 6, pp. 829-839.

Purves, D. 2012, *Neuroscience,* 5th edn, Sinauer Associates, Sunderland, MA.

Rohas, L.M., St-Pierre, J., Uldry, M., Jager, S., Handschin, C. & Spiegelman, B.M. 2007, "A fundamental system of cellular energy homeostasis regulated by PGC-1alpha", *Proceedings of the National Academy of Sciences of the United States of America,* vol. 104, no. 19, pp. 7933-7938.

Scarpulla, R.C. 2011, "Metabolic control of mitochondrial biogenesis through the PGC-1 family regulatory network", *Biochimica et biophysica acta,* vol. 1813, no. 7, pp. 1269-1278.

Scarpulla, R.C. 2006, "Nuclear control of respiratory gene expression in mammalian cells", *Journal of cellular biochemistry,* vol. 97, no. 4, pp. 673-683.

Scarpulla, R.C. 2002, "Nuclear activators and coactivators in mammalian mitochondrial biogenesis", *Biochimica et biophysica acta,* vol. 1576, no. 1-2, pp. 1-14.

Schapira, A.H. 2009, "Etiology and pathogenesis of Parkinson disease", *Neurologic clinics,* vol. 27, no. 3, pp. 583-603, v.

Schapira, A.H. 2008, "Mitochondria in the aetiology and pathogenesis of Parkinson's disease", *Lancet neurology,* vol. 7, no. 1, pp. 97-109.

Schapira, A.H., Agid, Y., Barone, P., Jenner, P., Lemke, M.R., Poewe, W., Rascol, O., Reichmann, H. & Tolosa, E. 2009, "Perspectives on recent advances in the understanding and treatment of Parkinson's disease", *European journal of neurology : the official journal of the European Federation of Neurological Societies,* vol. 16, no. 10, pp. 1090-1099.

Schmittgen, T.D. & Livak, K.J. 2008, "Analyzing real-time PCR data by the comparative C(T) method", *Nature protocols,* vol. 3, no. 6, pp. 1101-1108.

Schon, E.A. & Przedborski, S. 2011, "Mitochondria: the next (neurode)generation", *Neuron,* vol. 70, no. 6, pp. 1033-1053.

Schulz, J.B., Lindenau, J., Seyfried, J. & Dichgans, J. 2000, "Glutathione, oxidative stress and neurodegeneration", *European journal of biochemistry / FEBS,* vol. 267, no. 16, pp. 4904-4911.

Soriano, F.X., Leveille, F., Papadia, S., Bell, K.F., Puddifoot, C. & Hardingham, G.E. 2011, "Neuronal activity controls the antagonistic balance between peroxisome proliferator-activated receptor-gamma coactivator-1alpha and silencing mediator of retinoic acid and thyroid hormone receptors in regulating antioxidant defenses", *Antioxidants & redox signaling,* vol. 14, no. 8, pp. 1425-1436.

Spina, M.B. & Cohen, G. 1989, "Dopamine turnover and glutathione oxidation: implications for Parkinson disease", *Proceedings of the National Academy of Sciences of the United States of America,* vol. 86, no. 4, pp. 1398-1400.

Srinivasan, S. & Avadhani, N.G. 2012, "Cytochrome c oxidase dysfunction in oxidative stress", *Free radical biology & medicine,* vol. 53, no. 6, pp. 1252-1263.

St-Pierre, J., Drori, S., Uldry, M., Silvaggi, J.M., Rhee, J., Jager, S., Handschin, C., Zheng, K., Lin, J., Yang, W., Simon, D.K., Bachoo, R. & Spiegelman, B.M. 2006, "Suppression of reactive oxygen species and neurodegeneration by the PGC-1 transcriptional coactivators", *Cell,* vol. 127, no. 2, pp. 397-408.

St-Pierre, J., Lin, J., Krauss, S., Tarr, P.T., Yang, R., Newgard, C.B. & Spiegelman, B.M. 2003, "Bioenergetic analysis of peroxisome proliferator-activated receptor gamma coactivators 1alpha and 1beta (PGC-1alpha and PGC-1beta) in muscle cells", *The Journal of biological chemistry,* vol. 278, no. 29, pp. 26597-26603.

Surmeier, D.J., Guzman, J.N., Sanchez-Padilla, J. & Goldberg, J.A. 2011, "The origins of oxidant stress in Parkinson's disease and therapeutic strategies", *Antioxidants & redox signaling*, vol. 14, no. 7, pp. 1289-1301.

Thomas, B. & Beal, M.F. 2011, "Molecular insights into Parkinson's disease", *F1000 medicine reports*, vol. 3, pp. 7-7. Epub 2011 Apr 1.

Thomas, B. & Beal, M.F. 2007, "Parkinson's disease", *Human molecular genetics*, vol. 16 Spec No. 2, pp. R183-94.

Tritos, N.A., Mastaitis, J.W., Kokkotou, E.G., Puigserver, P., Spiegelman, B.M. & Maratos-Flier, E. 2003, "Characterization of the peroxisome proliferator activated receptor coactivator 1 alpha (PGC 1alpha) expression in the murine brain", *Brain research*, vol. 961, no. 2, pp. 255-260.

Tsunemi, T. & La Spada, A.R. 2012, "PGC-1alpha at the intersection of bioenergetics regulation and neuron function: from Huntington's disease to Parkinson's disease and beyond", *Progress in neurobiology*, vol. 97, no. 2, pp. 142-151.

Turrens, J.F. 2003, "Mitochondrial formation of reactive oxygen species", *The Journal of physiology*, vol. 552, no. Pt 2, pp. 335-344.

Valle, I., Alvarez-Barrientos, A., Arza, E., Lamas, S. & Monsalve, M. 2005, "PGC-1alpha regulates the mitochondrial antioxidant defense system in vascular endothelial cells", *Cardiovascular research*, vol. 66, no. 3, pp. 562-573.

VanGuilder, H.D., Vrana, K.E. & Freeman, W.M. 2008, "Twenty-five years of quantitative PCR for gene expression analysis", *BioTechniques*, vol. 44, no. 5, pp. 619-626.

Vidal, M., Morris, R., Grosveld, F. & Spanopoulou, E. 1990, "Tissue-specific control elements of the Thy-1 gene", *The EMBO journal*, vol. 9, no. 3, pp. 833-840.

Wang, Q., Yu, S., Simonyi, A., Sun, G.Y. & Sun, A.Y. 2005, "Kainic acid-mediated excitotoxicity as a model for neurodegeneration", *Molecular neurobiology*, vol. 31, no. 1-3, pp. 3-16.

Wareski, P., Vaarmann, A., Choubey, V., Safiulina, D., Liiv, J., Kuum, M. & Kaasik, A. 2009, "PGC-1{alpha} and PGC-1{beta} regulate mitochondrial density in neurons", *The Journal of biological chemistry*, vol. 284, no. 32, pp. 21379-21385.

Winklhofer, K.F. & Haass, C. 2010, "Mitochondrial dysfunction in Parkinson's disease", *Biochimica et biophysica acta*, vol. 1802, no. 1, pp. 29-44.

Wu, X., Wu, Z., Ning, G., Guo, Y., Ali, R., Macdonald, R.L., De Blas, A.L., Luscher, B. & Chen, G. 2012, "gamma-Aminobutyric acid type A (GABAA) receptor alpha subunits play a direct role in synaptic versus extrasynaptic targeting", *The Journal of biological chemistry*, vol. 287, no. 33, pp. 27417-27430.

Wu, Z., Puigserver, P., Andersson, U., Zhang, C., Adelmant, G., Mootha, V., Troy, A., Cinti, S., Lowell, B., Scarpulla, R.C. & Spiegelman, B.M. 1999, "Mechanisms controlling mitochondrial biogenesis and respiration through the thermogenic coactivator PGC-1", *Cell*, vol. 98, no. 1, pp. 115-124.

Zheng, B., Liao, Z., Locascio, J.J., Lesniak, K.A., Roderick, S.S., Watt, M.L., Eklund, A.C., Zhang-James, Y., Kim, P.D., Hauser, M.A., Grunblatt, E., Moran, L.B., Mandel, S.A., Riederer, P., Miller, R.M., Federoff, H.J., Wullner, U., Papapetropoulos, S., Youdim, M.B., Cantuti-Castelvetri, I., Young, A.B., Vance, J.M., Davis, R.L., Hedreen, J.C., Adler, C.H., Beach, T.G., Graeber, M.B., Middleton, F.A., Rochet, J.C., Scherzer, C.R. & Global PD Gene Expression (GPEX) Consortium 2010, "PGC-1alpha, a potential therapeutic target for early intervention in Parkinson's disease", *Science translational medicine*, vol. 2, no. 52, pp. 52ra73.

Zigmond, M.J., Hastings, T.G. & Perez, R.G. 2002, "Increased dopamine turnover after partial loss of dopaminergic neurons: compensation or toxicity?", *Parkinsonism & related disorders*, vol. 8, no. 6, pp. 389-393.

Acknowledgements

This Master's Thesis study was conducted at the Department of Biochemistry and Developmental Biology, Institute of Biomedicine, University of Helsinki, and in part at Minerva Foundation Institute for Medical Research.

I would like to thank Prof. Dan Lindholm for the opportunity to work in his group and to be part of this interesting project. I am very grateful for supervision and endless optimism during this Master's Thesis project.

Furthermore, I would like to thank Johanna Mäkelä for support and practical advice, as well as for many helpful discussions about my project, antioxidants, and chocolate, and for taking care of my NAD^+ levels.

Dr. Tho Huu Ho has been of invaluable help with any qPCR related questions. I am very grateful for lots of incredibly friendly advice.

I would like to thank my family and friends, who are absolutely *wunderbar*, for always being there for me and making life so worth living. Especially, I would like to thank my parents for their love and support throughout the years, and for always believing in me and my plans.

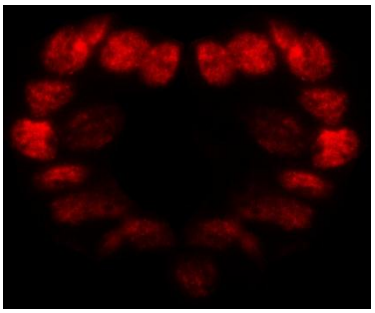

Figure 30 Love for PGC-1α.

Immunostaining for PGC-1α in Hc of tg mice